3-31-2021

# Ion channel candidates mediating orexin neuropeptide actions on brainstem serotonergic neurons

Saqlain Javed

# Ion channel candidates mediating orexin neuropeptide actions on brainstem serotonergic neurons

Saqlain Javed

A Thesis in the program in Biochemistry and Molecular Biology
submitted to the faculty of the
Graduate School of Basic Medical Sciences
in Partial Fulfillment of the Requirements
for the Degree of Master of Science
at New York Medical College

2021

# Ion channel candidates mediating orexin neuropeptide actions on brainstem serotonergic neurons

Saqlain Javed

Christopher S. Leonard, Ph.D.
(Sponsor)

Weihua Huang, Ph.D.
(Reader)

Esther L. Sabban, Ph.D.
(Reader)

Date of approval

# Acknowledgments

First and foremost, I would like to thank my mentor Dr. Christopher Leonard. I greatly appreciate your guidance throughout my thesis process, and I am also thankful that you gave me the chance to be a part of your lab. I have learned a great deal from your guidance, which has greatly increased my research and laboratory skills. Thank you for the time you have taken out from your busy schedule to help me throughout this process.

I would also like to thank my readers Dr. Huang and Dr. Sabban, who have helped me throughout this process. I am thankful for the knowledge and skills Dr. Huang has taught me that has helped me complete my thesis. I also appreciate the multitude of question he has answered regarding my research and his patience and quick replies.

I am also extremely grateful to Elizabeth Berry and Nancy Molina, for taking time out of their busy PhD schedules to teach me. I especially want to thank Elizabeth, who has supervised me throughout my research and has taught me most of the laboratory skills. She has assisted me through each of my experiments and has clarified a multitude of questions I've had regarding my research.

Most importantly, I would like to thank my family, especially my parents, wife and son. I would not be here without their support, love and encouragement. My dad has encouraged me throughout my life to pursue my dreams and has never faltered in his support. Without my family's support, I do not think I would have achieved this much in my life and no amount of thanks will ever be enough.

I would also like to thank the Touro Student Fellowship Grant and the NIH grant R01-NS027881.

# Table of Contents

# List of Figures and Tables

# List of Abbreviations

| Abbreviation | Meaning |
|---|---|
| $[Ca^{2+}]_i$ | Intracellular calcium concentration |
| 5HT | Serotonin/ 5-hydroxytryptamine |
| ABC | Avidin-Biotin Complex |
| ACh | Acetylcholine |
| AHP | After hyperpolarization |
| ai-oeAHP | Apamin insensitive orexin enhanced afterhyperpolarization |
| AMPAR | Isoxazole propionic acid receptor |
| ASAP | Automated Single-cell Analysis Pipeline |
| BIM | cell-autonomous inducer of apoptosis in endothelial cells |
| BSA | Bovine Serum Albumin |
| CaSR | Calcium sensing receptor |
| CNS | Central Nervous System |
| CNS | Central nervous system |
| DE | Differentially expressed |
| DR | Dorsal Raphe |
| EDS | Excessive daytime sleepiness |
| FFA | Flufenamate |
| GEO | Gene Expression Omnibus |
| GPCR | G-protein coupled receptor |
| H202 | Hydrogen Peroxide |
| HCRT | Hypocretin/ Orexin |
| HCRTR1 | Hypocretin receptor 1 |
| HCRTR2 | Hypocretin receptor 2 |
| IoeAHP | orexin enhanced afterhyperpolarization current |
| Ip3 | Inositol triphosphate |
| LC | Locus Coeruleus |
| LH | Lateral Hypothalamus |
| LHA | Lateral Hypothalamic Area |
| $Mg^{2+}$ | Magnesium |
| MR | Median raphe |
| NCX | Sodium calcium exchanger |
| NMDAR | N-methyl-D-aspartate receptor |
| NSCC | Nonselective cation channel |
| OCT | Optimal cutting temperature compound |
| OX | Orexin |
| $OX_1R$ | Orexin 1 receptor |
| $OX_2R$ | Orexin 2 receptor |
| PBS | Phosphate Buffered Saline |
| pCPA | para-chlorophenyl alanine |
| PFC | Prefrontal cortex |
| PGO | Ponto geniculo occipital |
| PKC | Protein kinase C |

| | |
|---|---|
| PLC | Phospholipase C |
| PVN | Paraventricular thalamic nucleus |
| REM | Rapid eye movement |
| sAHP | Calcium dependent slow AHP |
| SK | Small conductance |
| STS | Serotonergic system |
| TARP | type I transmembrane AMPA receptor regulatory protein |
| TMN | tuberomammillary nucleus |
| TPM | Transcripts per Million |
| TRPC | Transient receptor potential channel |
| tSNE | t-distributed Stochastic Neighbor Embedding |
| VGCC | Voltage gated calcium channel |
| VTA | Ventral tegmental area |

**Abstract**

A loss of neurons that synthesize the neuropeptide orexin produces the sleep disorder narcolepsy with cataplexy in humans and other animals. How symptoms of this disorder arise is not well understood, but selectively restoring orexin actions at 5-HT DR neurons rescues key symptoms (cataplexy), suggesting normal orexin signaling is important at these neurons. To better understand how orexin acts on these neurons, our lab identified a set of novel orexin actions that appear mediated by unidentified cation-permeable ion channels. To narrow down the list of possible channels, we used a bioinformatics approach to compare published gene expression profiles of 5-HT neurons and cerebellar Purkinje neurons. These neurons, despite having different electrical properties and different orexin responses, have cation permeable ion channels.

By using the Amigo2 database, we selected calcium channels, glutamate receptors, histamine receptors, inositol 1,4,5-triphosphate (IP3) receptors, ryanodine receptors, transient receptor potential (TRP) channels, potassium channels and sodium channels for examination. We then processed single-cell RNA sequencing (scRNAseq) data available on NCBI for 32 serotonergic neurons (SRP064626; from the Dymecki lab at Harvard) and 32 Purkinje cells (Series GSE78424). Single-cell RNA sequencing for both 5-HT neurons and Purkinje neurons were conducted using Illumina HiSeq 2500.

After normalization of gene expression profiles of these 64 single cells and comparisons of gene expression levels between cell clusters and cell sub-clusters, we identified channels enriched in a subset of 5-HT neurons. Based on published channel properties and experimental data from our lab, we isolated 39 candidate channel genes, from which we selected the *Nalcn* gene for initial testing. *Nalcn* encodes a sodium leak and

G protein-coupled receptor activated channel that regulates the resting membrane potential and neuronal excitability. It was up-regulated in 5-HT neurons compared to Purkinje cells ($p = 1.6e-06$) and it produces a membrane current with some similarities to the current activated by orexin in these neurons.

Using a commercially available antibody, we used immunocytochemistry to determine if the channel protein is expressed in 5-HT DR neurons. We identified an effective concentration of the anti-Nalcn antibody to visualize the channel with light microscopy (using VIP as a chromogen) and immunofluorescence. We first confirmed there was Nalcn immunostaining in the DR, and then in 5-HT DR neurons using the mice that express tdTomato fluorescence in 5-HT neurons (Sert-Cre/dTom mice). To conduct functional studies, we intend to knockout the channel since there are no selective Nalcn antagonists available. We utilized $Nalcn^{FL/FL}$ mice in which the *Nalcn* gene was flanked by loxP sites that enables gene knockout by Cre-recombinase expression. We first confirmed that DR 5-HT neurons appear normal in these mice using immunofluorescence staining of tryptophan hydroxylase (TPH), the rate-limiting enzyme for serotonin biosynthesis, and then that Nalcn immunoreactivity was present in the DR of these mice.

Preliminary experiments to knock out *Nalcn* by delivering Cre-recombinase via viral injection (AAV-Cre) into the DR of $Nalcn^{FL/FL}$ mice are also described. Success with using this antibody to monitor the loss of Nalcn immunostaining will confirm antibody specificity and encourage future whole cell patch clamp experiments to functionally test if Nalcn mediates the Orexin A action on 5-HT DR neurons. Collectively, these results will advance our understanding of the neural mechanisms underlying cataplexy.

## A) Introduction and Background

### A.1 Orexin

Orexin peptides were first identified in 1998 due to a convergence of 2 independent research groups. Sutcliffe's group was studying genes expressed in the hypothalamus in relation to obesity. They isolated a series of cDNA clones that are expressed in the hypothalamus by subtractive hybridization (de Lecea et al., 1998). Subtractive hybridization allows comparison of genes expressed at different stages of a biological process (Byers et al., 2000). Sutcliffe's group discovered a secretory protein of 130 amino acids which gave rise to 2 peptide products of similar structural characteristics. They named these peptides hypocretin 1 and hypocretin 2, due to it being expressed in the hypothalamus and its similarity to secretin (de Lecea et al., 1998). Around the same time, another group, using reverse pharmacology, identified 2 peptides, they named orexin A and orexin B, as the endogenous ligands of 2 orphan G-protein coupled receptors (GPCRs) (Sakurai et al., 1998) they named orexin receptor 1 ($OX_1R$) and orexin receptor 2 ($OX_2R$). These peptides are cleaved from prepro-orexin, which is a single precursor polypeptide expressed by a population of neurons clustered around the perifornical lateral hypothalamus (Sakurai et al., 1998). Later on, it was discovered that prepro-orexin and prepro-hypocretin were identical and that orexin-A and -B corresponded to hypocretin-1 and -2, respectively.

### A.2 Orexin and Narcolepsy

After the discovery of orexin, studies utilizing dog forward genetics and mouse reverse genetics increased our understanding of hypocretin biology, which further enhanced our knowledge of narcolepsy-cataplexy. Human narcolepsy-cataplexy is a

neurological disorder characterized by excessive daytime sleepiness, premature transition of REM sleep, and cataplexy (Aldrich, 1998; Bassetti & Aldrich, 1996). Narcolepsy is not a leading cause of death worldwide, but it is a disorder that is very debilitating. It affects both sexes equally and individuals with this disorder are known to have a very poor quality of life, sometimes even worse than patients that have epilepsy or Parkinson's disease (Beusterien et al., 1999; Teixeira et al., 2004). There are 2 major types of narcolepsy, which are type 1 and type 2. Individuals with type 1 narcolepsy, or narcolepsy with cataplexy have either low levels of the neuropeptide hypocretin or have cataplexy and excessive daytime sleepiness (EDS). Most individuals with narcolepsy and cataplexy have very low hypocretin-1 levels in the cerebrospinal fluid (Zawilska et al., 2012). Type 2 narcolepsy is also known as narcolepsy without cataplexy and individuals with this experience excessive daytime sleepiness but usually do not have muscle weakness triggered by emotion.

Cataplexy is a sudden loss of muscle tone while an individual is awake, which leads to weakness and a loss of muscle control. It is a major symptom of narcolepsy type 1 and is often triggered by sudden, strong emotions such as laughter, fear, anger, or excitement. Cataplexy is known to result from the loss of hypocretin containing neurons in the lateral hypothalamus (LH) (Reading, 2019). Cataplexy symptoms may sometimes appear years after the onset of excessive daytime sleepiness. Cataplectic attacks can range from one attack in a lifetime to daily attacks depending on the individual. Cataplexy can severely limit daily activities. Cataplexy is characterized by abrupt facial involvement during laughter behavior (Pizza et al., 2018). The worse cataplectic attacks can result in a complete body collapse which renders individuals unable to move, speak, or keep their

eyes open. The symptoms of cataplexy differ between adults and children. A defining aspect of cataplexy is that certain emotional stimuli usually trigger the episodes (Reading, 2019). It is known that cataplexy is caused by a severe loss of orexin neurons (Mahoney et al., 2019), but the exact mechanism that leads to cataplexy is unknown. Although, it is hypothesized that it might result from intrusion of REM sleep paralysis (atonia) into wakefulness (Pintwala & Peever, 2017).

Yanagisawa's group further investigated the role of Orexin in feeding by constructing a null mutant mouse that didn't produce either orexin peptide. They observed a reduced food intake in these mice, as expected, but they also observed that these mice would often abruptly cease movement (cataplectic attack) (Chemelli et al., 1999). They further researched this phenomenon by creating mice lacking either of the 2 orexin receptors. Their overall conclusion was that mice lacking orexin-2 receptor experienced slow cessations of movement that they concluded were sleep attacks (Chemelli et al., 1999). Around the same time, another group was successful in identifying mutations in the $OX_2R$ gene responsible for canine narcolepsy-cataplexy by positional cloning (Lin et al., 1999). Positional cloning is a technique that allows us to locate the position of a disease association gene along the chromosome (Puliti et al., 2007). It was also shown later on that orexin knock out (KO) mice were more greatly affected with cataplexy like attacks of rapid eye movement (REM) sleep than were $OX_2R$ KO mice (Willie et al., 2003).

**A.3 Localization of Orexin**

Orexin neurons regulate a wide range of physiological phenomena, like wakefulness, feeding, reward and thermogenesis (Inutsuka & Yamanaka, 2013). Orexin containing neurons are localized in the lateral hypothalamic area (LHA), although they

have widespread projections throughout the brain (Peyron et al., 1998). To identify the functional neuronal network, learning about the distribution pattern of orexin receptors could be essential. The action of orexin A and B are mediated by 2 receptors, which are Orexin 1 ($OX_1R$) and orexin 2 ($OX_2R$) receptors (also known as HCRTR1 and HCRTR2). $OX_1R$ has a much greater affinity for orexin A than it does for orexin B. Compared to that, orexin A and orexin B bind orexin 2 receptor with similar affinities (Sakurai et al., 1998). Both orexin 1 and orexin 2 receptor are G-protein coupled receptors, which transmit information into cells by activating G-protein, composed of alpha, beta, and gamma subunits (Gautam et al., 1998; Hepler & Gilman, 1992). It has been demonstrated, using in situ hybridization, that $OX_1R$ and $OX_2R$ differ in distribution (Marcus et al., 2001). A study was done in 2003 to examine the signal transduction pathway of orexin receptors in a neuronal cell line. This was done by transfecting OX1R and OX2R into a nerve-like BIM cell line. The study showed that in BIM/OX1R and BIM/OX2R cells, orexin induced an increase in (Ekholm et al., 2007). in a dose-dependent manner and orexin A had a higher potency on the effect of the (Ekholm et al., 2007). increase than did orexin-B in BIM/OX1R cells (Zhu et al., 2003).

$OX_1R$ mRNA has been observed in many brain regions including the hippocampus, paraventricular thalamic nucleus (PVN), ventromedial hypothalamic nucleus, dorsal raphe (DR) and locus coeruleus (LC). $OX_2R$ mRNA has been observed in a similar distribution including the cerebral cortex, hippocampus, DR, and many hypothalamic nuclei (Marcus et al., 2001). Among these regions, the DR and LC are well known to be involved in the maintenance of the awake state. The lateral hypothalamic (LH) orexin producing neurons

are an important part of promoting arousal and maintain wakefulness (Alexandre et al., 2013).

**A.4 Orexin Signaling**

Orexin signaling plays an important role in the maintenance of wakefulness. It has been shown that mice lacking orexin peptides, orexin neurons, or orexin receptors show human narcolepsy phenotypes (Hondo et al., 2010; Sakurai, 2007). Locus Coeruleus (LC) noradrenergic neurons has been a likely candidate to prevent cataplexy due to various studies that show cataplexy in humans and dogs is strongly suppressed by drugs that increase noradrenergic tone and is worsened by drugs that block noradrenergic tone (Hirai & Nishino, 2011; Nishino & Mignot, 1997). Recently, It has also been found that cataplexy like episodes can be inhibited by targeted restoration of orexin receptor expression in the DR and in the LC of mice lacking orexin receptors (Hasegawa et al., 2014). This suggests that the activation of LC noradrenergic neurons is not sufficient to suppress cataplexy in narcoleptic mice (Hasegawa et al., 2014).

Orexin peptides are synthesized by a small group of neurons in the hypothalamus (de Lecea et al., 1998) and are widely distributed in the central nervous system (CNS) (Peyron et al., 1998). The CNS is one of the most important orexin target tissue and the CNS neurons are the most investigated cells for orexin responses. Orexins are shown to produce a slow and long-lasting depolarization that can be large enough to initiate firing of a neuron. Orexin receptors couple to effectors that produce depolarization, whose molecular identity is generally not known, and are known as excitatory neuropeptides (Leonard & Kukkonen, 2013). The depolarization is usually attributed to the closure of $K^+$ channels active at rest, activation of an electrogenic sodium-calcium exchanger (NCX),

and the activation of non-selective cation channels (NSCCs) (Eriksson et al., 2001; Horvath et al., 1999; Hwang et al., 2001).

**A.5 The Dorsal Raphe**

A chemical present in abundance in the dorsal raphe is serotonin (5-HT). 5-HT is an essential chemical that is found in all organs in mammals, such as brain, lungs, liver, kidney and skin. The distribution of 5-HT is widespread in the brain and it regulate the activity of nearly all brain regions. This is why 5-HT has been implicated in a variety of brain functions, some of which are the sleep-wake cycle, hormonal regulation, and appetite (Nakamura, 2013). There has been much controversy on the role of 5-HT in sleep. The first hypothesized sleep-promoting substance of modern neuroscience was 5-HT. It was reported in 1955 that reserpine could decrease cerebral 5-HT and induce sedation or a "sleep like state" (Brodie et al., 1955). This was the first time that sleep and serotonin were mentioned together in a paper. Then in 1965, it was discovered that the administration of reserpine could trigger the continuous appearance of Ponto geniculo occipital (PGO) activity, even during waking (Jouvet-Mounier et al., 1965). PGO waves are biphasic field potentials that are identified in a wide range of mammals, which are related to sleep and are known to be identified in waking perception and eye movement. It is also known that PGO waves are early predictors for the onset of REM sleep (Gott et al., 2017). It has also been shown that the action of reserpine was blocked by the monoamine oxidase inhibitors, pheniprazine, harmaline and clorgyline (Gershon & Brooks, 1976).

In the central nervous system (CNS), the raphe is a diffuse network of brainstem nuclei, that synthesizes 5-HT and send projections to almost every region of the brain (Azmitia & Segal, 1978). Studies have shown that ablation of the raphe in cats reduced

serotonin levels and sleep, in proportion to the size of the lesion (Jouvet, 1968). It has also been shown that intraperitoneal injections of para-chlorophenyl alanine (pCPA) also reduced sleep (Koella et al., 1968). These studies gave rise to the theory of sleep, in which serotonin plays an important sleep-promoting role. Additional finding show that serotonergic raphe neurons are active during wakefulness, less active during non-rapid eye movement (NREM) sleep, and mostly silent during rapid eye movement (REM) sleep further support a wake-promoting role for serotonin and the raphe (McGinty & Harper, 1976).

Serotonergic neurons in the dorsal raphe nucleus (DRN) play important roles in many physiological processes such as sleep/arousal, mood control, and regulation of food intake (Leibowitz & Alexander, 1998). Orexin A is known to strongly excite dorsal raphe (DR) serotonergic neurons, which is shown by studies done in vitro (Brown et al., 2001). It has also been shown that the lateral hypothalamus-raphe connection mediated by orexin A might contribute to a negative feedback loop regulating food intake. The release of orexin A in various hypothalamic and brainstem nuclei elicit feeding but also excite serotonin neurons, which results in an enhanced release of serotonin in the ventromedial hypothalamus (Leibowitz & Alexander, 1998; Sakurai et al., 1998). Along with the regulation of food intake, these results by brown show an importance in the context of narcolepsy. In narcolepsy, REM sleep episodes intrude into normal waking and serotonin has a suppressive effect on REM sleep generation (Jacobs & Fornal, 1999). Orexin signaling in DRN 5-HT neurons appears critical for the suppression of cataplexy.

### A.6 Orexin and calcium channels

A major response upon the activation of orexin receptor is $Ca^{2+}$ influx, which leads to the amplification of other responses mediated by orexin receptors (Sakurai et al., 1998). PLC activation and the binding of OX1R and OX2R are strongly dependent on the extracellular $Ca^{2+}$ concentration. It is shown in a study that when $Ca^{2+}$ entry is reduced by depolarizing the cells or by inhibiting the receptor-operated $Ca^{2+}$ channels, orexin A stimulated Phospholipase C activity was much more strongly inhibited than orexin A binding (Putula et al., 2014). This suggests to us that calcium plays a double role in orexin signaling by amplifying orexin signals via $Ca^{2+}$ influx and being a prerequisite for both ligand-receptor interaction (Putula et al., 2014). Orexin is known to increase the intracellular calcium concentration in expression systems. It is known that both $OX_1$ and $OX_2$ receptors release $Ca^{2+}$ from intracellular stores and that a primary $Ca^{2+}$ influx is evoked at lower orexin concentrations (Kukkonen & Leonard, 2013). Orexin receptors throughout the CNS are known to drive membrane depolarization and increase the intracellular $Ca^{2+}$ levels (Leonard & Kukkonen, 2013). Orexin is known to modulate calcium in the DR (Kukkonen & Leonard, 2013; Liu et al., 2002). The application of orexin is also known to produce membrane depolarization and action potential in DR neurons (Brown et al., 2002; Burlet et al., 2002). Orexin is also known to elicit $Ca^{2+}$ transients in the soma and dendrites of neurons in the dorsal raphe (Kohlmeier et al., 2004; Kohlmeier et al., 2008). It is also shown that Orexin A (OXA) enhances a late afterhyperpolarization (AHP) in serotonergic neurons which is $Ca^{2+}$ dependent (Ishibashi et al., 2016). Recently, it has been seen that extracellular calcium also block the orexin mediated inward current (Leonard lab Figure 6, unpublished)

### A.7 Orexin and glutamate receptors

Orexin A administration is known to modulate glutamatergic thalamocortical synapses and facilitates attention (Lambe et al., 2005). Also, in the hippocampus, orexin A is known to modulate synaptic plasticity through coordinated modulation of cholinergic, GABAergic, glutamatergic, and noradrenergic signaling (Selbach et al., 2004). It is also shown in a study that the administration of Orexin A, rapidly and significantly increases ACh and glutamate within the PFC (Calva et al., 2018). Orexin A is also known to colocalize with glutamate (Torrealba et al., 2003). Glutamate receptor modulation by orexin signaling is also shown in the ventral tegmental area (VTA), where orexin is shown to increase N-methyl-D-aspartate receptors (NMDARs), which leads to increased AMPAR/NMDAR ratio (Borgland et al., 2006). AMPA and NMDA are shown to increase the 5-HT neuronal firing in the DRN (Gartside et al., 2007). Studies have also shown that agonists of ionotropic glutamate receptors have activated orexin neurons and that glutamate antagonists have reduced their activity (Li et al., 2002; Yamanaka et al., 2003). This suggests that orexin neurons are tonically activated by glutamate.

### A.8 Orexin and histamine effectors

The enhancement of orexinergic system through the Orexin 2 receptors is known to excite the histaminergic system (Eriksson et al., 2001). Histaminergic neurons are localized to the tuberomammillary nucleus (TMN) of the posterior hypothalamus and send extensive projections throughout the CNS (Wada et al., 1991). The TMN also predominantly expresses orexin 2 receptors (Eriksson et al., 2001), which has an affinity to bind orexin A (Sakurai et al., 1998). Increases of histamine concentration in the hypothalamus has been

shown to help excessive daytime sleepiness in narcolepsy and also help cataplexy control (Reading, 2019).

**A.9 Orexin and ryanodine receptors**

Functional coupling between IP3R and RyR could be a critical component of intracellular $Ca^{2+}$ signaling in many excitable cells (Tjondrokoesoemo et al., 2013). The activation of IP3 receptor in response to cAMP signaling is a PKA-dependent mechanism and the activation of ryanodine receptors is an EPAC dependent mechanism (Kang et al., 2003; Tsuboi et al., 2003). It is shown in a study that Orexin A potentiated glucose-stimulated insulin secretion, which increases $[Ca^{2+}]_i$ levels, through adenylate cyclase and ryanodine receptor activation (Park et al., 2015). Activation of ryanodine receptors and $Ca^{2+}$ release from intracellular stores is shown to enhance the SK component of the oeAHP (Ishibashi et al., 2016). It is also shown in this study that the activation of IP3 receptors might not be necessary or sufficient.

**A.10 Orexin and TRP channels**

The transient receptor potential (TRP) protein superfamily is a diverse group of ion channels that consist of 28 cation permeable channels that are grouped into 6 subfamilies (Samanta et al., 2018). These channels show great diversity in activation, inhibition and selectivity of ion conductance. TRP cation channels are known to mediate the flux of $Na^{+}$ and $Ca^{2+}$ across the plasma membrane and into the cytoplasm (Song & Yuan, 2010). It has been shown that TRP channels are activated by G-protein coupled receptors (GPCRs) or receptor tyrosine kinases (Plant & Schaefer, 2003; Trebak et al., 2007). The TRP channels are $Na^{2+}$ permeable channels that are mediated by Orexin. Studies have shown that Transient receptor potential channel 3 (TRPC3) is activated when orexin A act on Orexin 1

receptor, thus triggering $Ca^{2+}$ responses (Peltonen et al., 2009). This suggest that a change in calcium levels is not necessarily mediated through G-protein Coupled receptors (GPCRs) and that orexin receptors activate a novel mechanism of $[Ca^{2+}]_i$ elevation through nonselective cation channels (NSCCs) (Wang et al., 2018). Orexin signaling is also known to activate the mTORC1 pathway, which is triggered by the lysosomal v-ATPase pathway, which is dependent on transient cytoplasmic calcium (Wang et al., 2014).

**A.11 Orexin and potassium channels**

Orexin neurons are inhibited by an increase in temperature, which is mediated by ATP-sensitive potassium (KATP) channels (Parsons et al., 2012). Two-pore domain potassium channels become activated with increasing temperatures in cerebellar granule neurons and dorsal root ganglion neurons (Kang et al., 2005). ATP-sensitive $K^+$ channels are also known to mediate lactate effect on orexin neurons (Parsons & Hirasawa, 2010) and Extracellular lactate concentration is known to be a reliable sleep/wake biomarker (Naylor et al., 2012). Orexin neurons are also known to be inhibited by glucose. This inhibited is mediated by tandem-pore $K^+$ ($K_{2p}$) channels (Burdakov et al., 2006).

**A.12 Orexin actions on the DR**

Orexin has been shown to have more complex effects in the DR, but like the remaining CNS, the molecular identity of the effectors is not known. In addition to producing membrane depolarization, orexin A (OXA) enhances a late afterhyperpolarization (AHP) in serotonergic neurons and this orexin enhanced AHP (oeAHP) is $Ca^{2+}$ dependent.(Ishibashi et al., 2016). Functionally, the AHP is a feedback mechanism that shapes the firing frequency and firing pattern in many types of neurons

(Duménieu et al., 2015). The Modulation of the AHP represents an important mechanism by which excitability of a neuron can be regulated (Burrell & Crisp, 2008).

The orexin effect on the DR slow AHP is illustrated in Figure 1. Application of orexin produces an inward current (downward shift in the trace) that depolarizes 5-HT DR (**Figure 1A**). The vertical transients indicate brief test pulses to activate the AHP. These current quickly settle to baseline before orexin is applied but then get larger and slowly settle to baseline after orexin is applied (dotted box) indicating the AHP current has been enhanced by orexin (IoeAHP). Looking on a faster time scale (**Figure 1B**), there are 2 parts to the IoeAHP, one of which is a slow decaying part that was not blocked by apamin and the second is a faster decaying part that was blocked by apamin. This indicates that the fast part is mediated by SK-type $Ca^{2+}$ -activated $K^{+}$ channels. The apamin insensitive part (Iai-oeAHP) was consistently about half the size of the inward current which suggest that these currents may be linked (Ishibashi et al., 2016; Ishibashi and Leonard, unpublished observations). Several lines of evidence suggest that the slower decaying, apamin insensitive current results from $Ca^{2+}$ influx that transiently closes the very cation channel(s) activated by orexin. One way this could happen in 5-HT DR neurons is illustrated in the schematic below (**Figure 1C**). In this scheme, either OX1R or OX2R activation is sufficient to induce the inward current and the oeAHP by activation of PLC. This activates one or more types of non-selective cation channels (NSCCs) through unknown signals, but without involvement of the SER $Ca^{2+}$ -stores, RyRs or IP3Rs (Ishibashi et al., 2016). A transient influx of $Ca^{2+}$ through voltage-gated $Ca^{2+}$ channels is sufficient to transiently reduce the inward current (NSCC) by about half after binding to an unidentified neuronal Ca2+ sensor protein (NCS), thereby producing the novel ai-oeAHP.

In this scheme the NSCC plays a pivotal role in both orexin excitation and in the oeAHP. Since the molecular identity of the NSCC is not known, it will be of significant interest to determine the NSCCs expressed in 5-HT DR neurons.

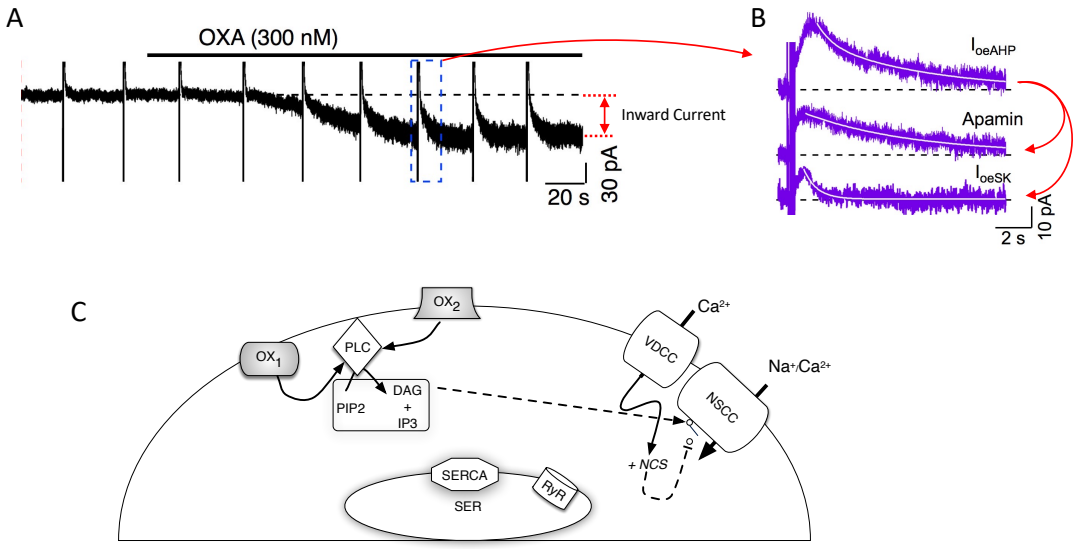


**Figure 1 | OXA produces an inward current that depolarizes serotonergic DR neurons and also enhances a novel late AHP which is likely mediated by the closure of the cation channels carrying the inward current.**
**A)** OXA application induces a large noisy inward current. The AHP was periodically tested by delivering 5 brief (10 ms) depolarizations to +10 mv at 20 Hz (vertical transients). Prior to OXA, the membrane current quickly settled to baseline. After OXA, a slow outward current, termed the IoeAHP, followed these pulses (blue box). **B)** The IoeAHP (top trace) was composed of two components: a slower decaying part that was not blocked by apamin (Apamin; middle trace) which is termed the apamin-insensitive oeAHP (Iai-oeAHP) and a faster decaying part that was blocked by apamin (bottom trace) indicating it was mediated by SK-type $Ca^{2+}$ -activated $K^+$ channels. Modified from Ishibashi et al., 2016. **C)** A schematic summarizing our working hypothesis for the ai-oeAHP. This is based on the data above and other data obtained in the Leonard Lab (Ishibashi and Leonard, unpublished observations).

As noted in Ishibashi et al (2016), the functional impact of the oeAHP is to alter the firing properties of 5-HT DR neurons so as to reduce tonic firing without attenuating transient firing during active waking, when orexin is released. The loss of orexin in narcolepsy would degrade these firing changes and may contribute to the narcolepsy phenotype.

With these data in mind, the work described here will use a combination of bioinformatics and knockout approaches to identify some potential candidate effectors mediating the action of orexin in serotonergic DR neurons.

**A.13 Single-cell RNA sequencing**

Single-cell RNA sequencing (scRNA-seq) is a powerful tool for transcriptome analysis that can measure the distribution of expression levels for each gene across a population of cells (Parsons et al., 2012). scRNA-seq allows comparison of individual cell transcriptome, which is why it has been used to assess transcriptional similarities and differences within a population of cells (Haque et al., 2017). The assessment of transcriptional differences between individual cells can be used to identify rare cell populations (Parsons & Hirasawa, 2010), like malignant tumor cells in a tumor mass (Naylor et al., 2012). scRNA-seq is also being used to trace developmental relationships between heterogenous, yet related, cellular states in scenarios such as lung epithelial differentiation (Treutlein et al., 2014). In addition to this, scRNA-seq can also provide important information about essential characteristics of gene expression, such as monoallelic gene expression (Deng et al., 2014).

scRNA-seq can be very helpful in finding answers to research questions, but it's important to recognize that the answers can vary depending on the protocol used. RNA-seq is a great technique for the quantitative analysis of messenger RNA molecules in a biological sample (Haque et al., 2017). This is a useful approach for studying cellular responses. Before any analysis can be done, it is important to filter and normalize the data. Data normalization is important for RNA-seq because it addresses limitations presented by low amounts of material and various forms of bias in the sequencing process (Lytal et al.,

2020). There are several methods available for data normalization, some of which rely on spike-in genes, referring to the genes whose expression is higher in a certain subgroup (Vallejos et al., 2015).

### A.13.1 Clustering analysis

Clustering analysis is used to generate cell type-specific clusters by using cell type marker genes. The different types of clustering are unsupervised clustering, k-means clustering, hierarchical clustering, and graph-based clustering. Unsupervised clustering has been studied in machine learning and has many different applications. This type of clustering does not depend on predefined classes and training examples while classifying the data (Tasoulis et al., 2006). In k-means clustering, the cluster center is predetermined and each cell is assigned to the nearest cluster (James et al., 2013). Hierarchical clustering is the most popular method for gene expression analysis. In this method, genes with similar expression patterns are grouped together and are connected by a series of branches. Hierarchical clustering can also be used to group together experiments similar expression profiles (Pagnuco et al., 2017).

### A.13.2 Heat map analysis

Heat map is a great tool for visualizing complex statistical data, using colors to represent values. It shows magnitude of expression as color in two dimensions. In a color intensity ranging from blue (no expression) to orange (highest expression), it shows how much or how little a specific gene is expressed in each cell. They are useful for visualizing the expression of genes across individual samples and are commonly used to visualize scRNA-seq results (Batut et al., 2018). To generate a heatmap, the gene counts need to be normalized for differences in sequencing depth and composition bias between the samples

(Batut et al., 2018). Sequencing depth refers to the average number of nucleotides contributing to a portion of an assembly, referring to how many times each base has been sequenced. Normalizing for composition bias takes into account certain genes that are very highly expressed in a group.

## B) Hypothesis and Specific Aims

### B.1 Hypothesis

The loss of orexin can result in the sleep disorder narcolepsy with cataplexy in humans and other animals. How symptoms of this disorder arise is not well understood, but selectively restoring orexin actions at 5-HT DR neurons rescues key symptoms (cataplexy), suggesting normal orexin signaling is important at these neurons (Hasegawa et al., 2014). To better understand how orexin acts on these neurons, our lab identified a set of novel orexin actions that appear mediated by unidentified cation-permeable ion channels. To narrow down the list of possible channels, we used a bioinformatics approach to compare published gene expression profiles of 5-HT neurons and cerebellar Purkinje neurons. These neurons, despite having different electrical properties and different orexin responses, have cation permeable ion channels.

### B.2 Specific Aims

#### B.2.1 Aim 1: Analysis of published gene profiles of serotonergic neurons and cerebellar Purkinje neurons.

Our lab previously identified a set of novel orexin actions that appear mediated by unidentified cation-permeable ion channels. After arriving with several groups of channels, using the Amigo2 database, we compared the gene expression profiles of the individual genes. For this we choose to compare serotonergic neurons with Purkinje cells, due to the difference in electrophysiology of both types of neurons. We processed and analyzed (using R) the single-cell RNA sequencing (scRNAseq) data available on NCBI for 32 serotonergic neurons (SRP064626; from the Dymecki lab at Harvard) and 32 Purkinje cells (Series GSE78424). Then the gene counts were separated depending on which group of

genes were needed for analysis. The 32 serotonergic cells were compared with the 32 Purkinje cells using R and an automated single cell analysis pipeline (ASAP).

### B.2.2 Aim 2: Testing a Candidate Ion channel

Based on the published channel properties, experimental data from our lab, and the scRNA-seq data analyzed, we identified 7 candidate channel genes, from which we selected the *Nalcn* gene for initial testing. *Nalcn* encodes a sodium leak and G protein-coupled receptor activated channel that regulates the resting membrane potential and neuronal excitability. It was up-regulated in 5-HT neurons compared to Purkinje cells ($p = 1.6e-06$) and it produces a membrane current with some similarities to the current activated by orexin in these neurons. It was first confirmed using immunostaining that Nalcn was present in the dorsal raphe. Then it was tested whether Nalcn was present in 5-HT DR neurons. After confirmation, the next step was to conduct functional studies, for which we intended to knockout the channel by injecting a GFP Cre virus into the DR of $Nalcn^{FL/FL}$ mice.

## C) Materials and Methods

### Aim 1: Analysis of published gene profiles of serotonergic neurons and cerebellar Purkinje neurons

### C.1 Processing raw scRNA-seq data

#### C.1.1 Obtaining scRNA-seq data

The scRNA-seq data used throughout this work was obtained from the Gene Expression Omnibus (GEO) database. The serotonergic neuron samples used were from the study "Multi-scale molecular deconstruction of the serotonin neuron system" (SRP064626) done by the Dymecki lab at Harvard Medical School (Okaty et al., 2015). Cells were obtained from manually sorted GFP-expressing neurons of triple transgenic En1::Cre, Pet1::Flpe, RC::PFtox male mice, from Dorsal Raphe. Then total RNA was recovered using picopure RNA isolation. Afterwards, the Nugen Ovation RNASeq system v2 was used for RT and linear amplification, which was followed by Covaris sonication and Nugen Ultralow for library preparation. Fifteen of the single cells obtained were from the dorsal raphe and 15 were from the median raphe. The cerebellar Purkinje neurons used were from mouse ENCODE project (Series GSE78424). The 32 samples were obtained from scRNA-seq of 20 excised and homogenized Purkinje neurons from male wild type C57Bl6 mice. The instrument used for the scRNA-seq of both serotonergic neurons and Purkinje neurons was Illumina HiSeq 2500. The SRR number (raw files) for all 64 cells were recorded in notebook.

#### C.1.2 Loading and saving raw scRNA-seq data

Each individual cell was processed separately. The raw file for each of the 64 cells was loaded onto a computer running Ubuntu Linux (version 16.04), using SRAtoolkit

(command: prefetch SRR##; version 8). Then the data was converted to fastq files (command: fastq-dump). Both SRA and fastq files were saved into a specified folder. This was repeated for all 64 cells and the fastq file for each cell was saved into a separate folder.

### C.1.3 Checking quality of reads

After obtaining scRNA-seq data, the quality of reads was checked using FastQC (version 0.11.9), which is a quality control tool for sequencing data. It takes input data and returns a report on read quality. Both reports of forward and reverse reads were checked for any flaws. Then the reads were trimmed using TRIM GALORE (version 0.5.0) to remove any adapters and/or low-quality sequences. After trimming, another FastQC report was generated to check the quality of the trimmed results. This new FastQC report showed that the reads pass the 'adaptor content' plot. Fastq is the raw reads of scRNA-seq data.

### C.1.4 Alignment of reads

After trimming the reads, the next step is to map them to a reference genome. This process is called alignment. The reference genome for *Mus musculus* was downloaded from Ensembl in GTF format (Ensembl release 102). Alignment is usually needed to quantify gene expression or find genes which are differentially expressed between samples. Kallisto (version 0.46.1) was used for pseudo-alignment of reads to the reference transcriptome (version GRCm38.91). Kallisto allows for pseudo-aligning reads from scRNA-seq experiments. Kallisto pseudo-aligns reads to a reference transcriptome rather than a reference genome and maps reads to splice isoforms rather than genes. The four output files from the kallisto alignment were saved to a specified folder.

### C.1.5 Construction of expression matrix

In an expression matrix, each column represents a cell, and each row of the expression matrix represents a gene. Each entry represents the expression level of a particular gene in a given cell, by which the expression is measured.

## C.2 Analysis of single cell RNA-seq data

### C.2.1 Categories of channels

After forming the gene counts with expression levels, they were saved in a worksheet in csv format. Different files were constructed for each category of channels that needed to be analyzed. The categories of channels and receptors selected were calcium, glutamate, histamine, ryanodine, TRP, and potassium. These list of genes from each category was constructed using the Amigo2 Gene Ontology (GO) database. Amigo2 was used to filter out and identify genes with certain parameters. The parameters entered to conduct the list of channels were ion channels, neurons, GPCR, calcium, glutamate, histamine, ryanodine, TRP, potassium, and non-voltage genes. This produced a list of a few hundred genes, which were separated into different classes of genes and analyzed. R (version 3.6.2) was initially used to visualize the gene expression of some channels to make sure the reads were properly processed. Further analysis of the groups of channel genes was done using ASAP.

### C.2.2 Filtering and Normalization

Before any analysis, the data were filtered and normalized. This was done separately for each group of channel genes using ASAP. The results were filtered using Transcripts per million reads (TPM).

Then the data was normalized to counteract any technical noise, due to imprecise measurements (Lytal et al., 2020) or biological variation attributed to the natural differences among the cells under the same biological condition (Kim et al., 2015). The goal of normalization is for the differences in the normalized read counts to represent differences in the true expression (Evans et al., 2018). Each class of genes that were analyzed were filtered and normalized separately.

### C.2.3 Cell clusters

After normalization, a t-distributed stochastic neighbor embedding (tSNE) plot was generated using k-means clustering with a perplexity of 21 and a theta of 0.5. tSNE is a dimension reducing method for visualizing high dimensional data. In the scRNA-seq data, it shows the gene expression measurements per cell in two dimensions. The plot is constructed in a way that when two cells are close in the lower dimension space, they are likely close in the higher dimension space as well. In the plot, only the relative distance between each cell (point) matter (Hollt et al., 2018). tSNE is primarily a visualization technique and that shows you how the data is arranged in a high dimensional space. Here, the tSNE plot showed two cell clusters which distinguished between the serotonergic neurons and the Purkinje neurons. In a tSNE plot, you set a low perplexity when you want a more local scale analysis and are only concerned about the few closest points. In our analysis, we used a high perplexity 21, which gives us a more overall picture (Hollt et al., 2018). So, with a high perplexity, it focuses on the overall group of cells, instead of each individual cell and its closest counterpart. To get the overall differentiation between serotonergic neurons and Purkinje cells, any perplexity value between 5 and 50 should work fine. For the tSNE plot, a lower theta value (between 0 and 1) was chosen because a

low value leads to a slower but finer approximation of the data. With a higher theta value, you would get a faster but coarser approximation (Hollt et al., 2018).

#### C.2.4 Heat maps

Heat maps for each category were generated using the normalized data of both serotonergic neurons and Purkinje neurons. Ward D2 clustering method was used to generate the heat maps to show the hierarchical clustering. The distance metric used was Euclidean.

#### C.2.5 Differential Expression (DE)

DE was done on each group of channel genes using Limma on ASAP. This was done on the filtered and normalized data. The false discovery rate (FDR) was set to less than or equal to 0.05. The fold change was set to more than or equal to 2. FDR is a method to determine the rate of type 1 errors in null hypothesis testing when doing multiple comparisons. Fold change is a value that shows how much a quantity changes between an original and a subsequent measurement.

### Aim 2: Testing a Candidate Ion channel

### C.3 Mice

Wildtype C57Blk6, Sert-Cre::dTom, and $Nalcn^{FL/FL}$ mice were utilized for all the experiments in this study. All strains were already available at NYMC comparative medicine. Mice were kept in a pathogen-free environment and all experiments were conducted on male mice who were at least 14 weeks of age. All animal procedures were conducted in accordance with the institutional animal care and use committee (IACUC) guidelines approved by New York Medical College.

### C.4 Cre Injection Surgery

Nalcn$^{FL/FL}$ mice were anesthetized using ketamine/xylazine cocktail and 300 ul of Cre virus was injected into the DR region (**Figure 2**). The Surgery was done using a stereotaxic (**Figure 3**) and the virus was injected nanoject 2. The DR location was mapped using the Angle2 z axis software and measuring Bregma and lambda. The AAV9 cre virus injected was pENN.AAV.hSyn.HI.eGFP-Cre.WPRE.SV40 (add gene 105540-AAV9; 1 x10 13 vg/ml). The pipettes used for the injection were 3.5-inch Drummond pipettes and were pulled on a Sutter P-95 horizontal pipette puller and broken back to tip diameters of 20-25um.

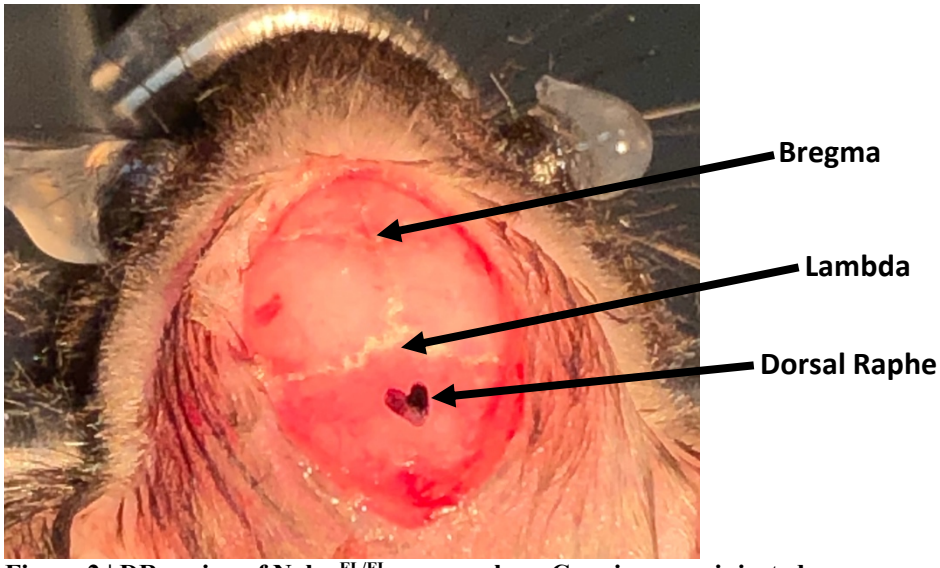


**Figure 2 | DR region of Nalcn$^{FL/FL}$ mouse where Cre virus was injected.**

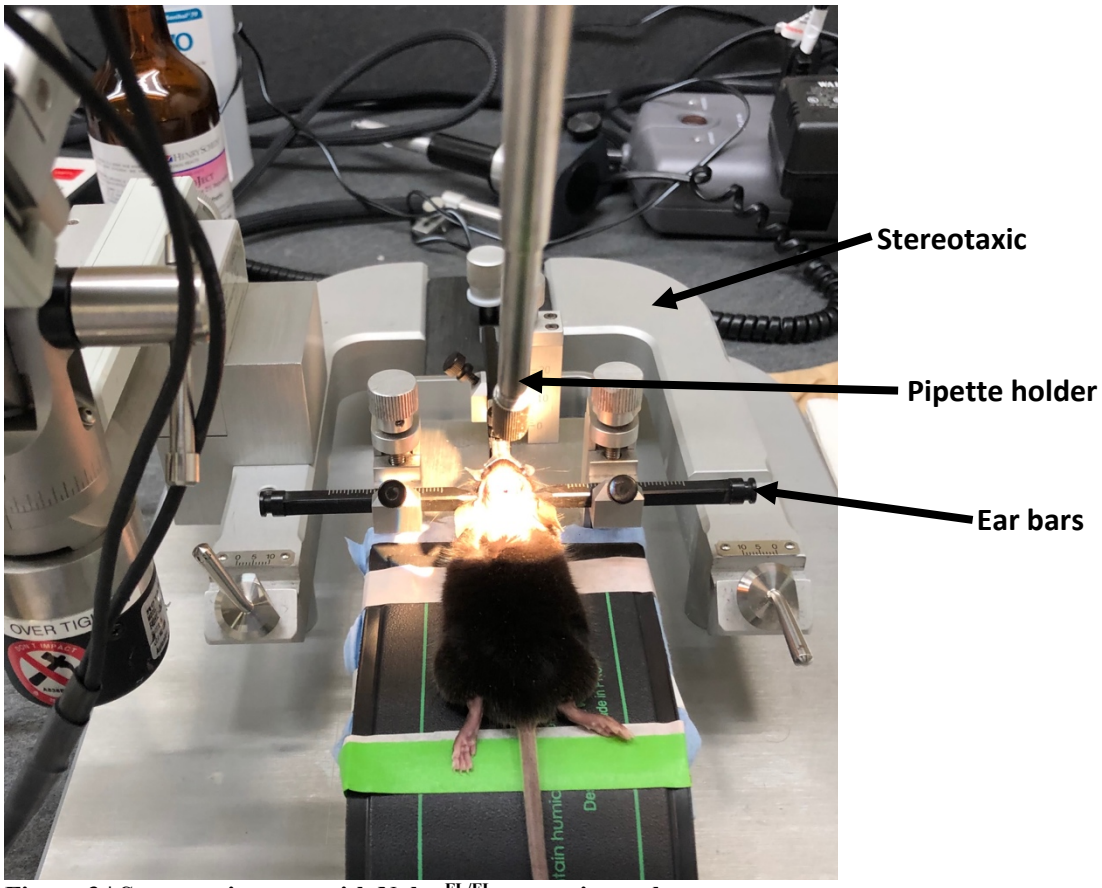


**Figure 3 | Stereotaxic setup with Nalcn$^{FL/FL}$ mouse in ear bars**
Mouse is placed in a heat pad and held onto stereotaxic by the ear bars with a Pipette holder pointed and the dorsal raphe region at 0 degrees, which contains a 25um thick pipette with GFP Cre virus inserted into it.

### C.5 Perfusions

Mice were deeply anesthetized using ketamine/xylazine cocktail and then perfused with 4% paraformaldehyde (PFA). Brains were then collected and placed in 4% PFA for 24 hours and then switched to 30% sucrose to cryopreserve the tissue.

### C.6 Sectioning Brains

Brains were flash frozen using methyl butane and then frozen in a cube of OCT. Brain sections (40um) of the DR were made using a Leica cryostat. Each section was collected separately and placed in a 24-well plate with 0.01M PBS solution.

### C.7 VIP Immunohistochemistry

On the first day, the desired sections were added to a 24-well plate and washed with 0.01M PBS for 15 minutes. Then the sections were incubated for 30 minutes in 500ul of 1% H202 in 0.01M PBS with continuous agitation. H202 was then removed, and the sections were washed with PBS for 15 minutes. Then the sections were blocked for non-specific binding with 500ul of 1% BSA/ 0.05% sodium azide/ 0.01M PBS solution for 45 mins with continuous agitation. At the end of day 1, 500ul of [1:100] Anti-Nalcn extracellular antibody (Lot#: ASC022AN0150; Cat #: ASC-022; Alomone labs) was added to the sections and they were left at 4 degrees Celsius for 2-night incubation with continuous agitation.

After 2-day incubation, the primary antibody was removed from the sections and they were washed with PBS for 100 minutes. Then the secondary antibody, 500ul of [1:200] biotinylated anti rabbit IgG (Lot#: ZD1113), was added to the sections and incubated for 60 minutes with continuous agitation. ABC solution was them prepared with 5ml PBS, 2 drops of Avidin DH, and 2 drops of biotinylated horse radish. Then, 500ul of the ABC solution was incubated for 30 mins and added to the sections, after they were washed with PBS for 15 minutes. The sections were incubated with ABC solution for 30 mins and then washed with PBS for 15 mins. 500ul of VIP solution was then prepared and added to the sections, individually, for around 3 mins until reaction. Then the sections were immediately washed with PBS to stop the reaction. The sections were then mounted on slides and dipped in newly made 80% EtOH for 1 minutes, 90% EtOH for 1 minutes, and 100% EtOH for 1 minute. Then the sections were dipped in xylene for 2 minutes and removed and to coverslip using permount.

### C.8 Immunofluorescence

Sections with cre expression were added to 24-well plate and washed with 0.01M PBS for 15 mins. Sections with cre expression were covered with foil during all steps. The sections were then blocked for non-specific binding in 500ul of 1%BSA/ 0.05% azide/0.01M PBS solution for 60 minutes. Then 500ul of [1:100] primary Nalcn antibody (Lot#: ASC022AN0150) was added to the sections and left at 4 degrees Celsius for 2-day incubation with continuous agitation and foil covering.

After 2-day incubation, the sections were washed for 100 minutes with continuous agitation. Then the sections were incubated in 500ul of secondary antibody, Alexa fluor 594 (Lot#: 1987293), for 45 minutes. the sections were then mounted, dried and cover slipped with 25ul of Vectashield.

### C.9 Microscopy

All images of brain sections were taken using a Keyence BZ-X800 fluorescent microscope under high resolution with 4X, 20X and 60X objectives.

## D) Results

### Aim 1: Analysis of published gene profiles of serotonergic neurons and cerebellar Purkinje neurons

### D.1 Analysis of gene profiles

scRNA-Seq data for 32 serotonergic neurons and 32 cerebellar Purkinje neurons were processed for comparison of gene expression levels between cell clusters and cell sub-clusters. Because of the difference in electrophysiology between serotonergic neurons and Purkinje cells, we expect the channel and receptor profiles to be strongly different between these cell types. These differences in conjunction with the known actions of orexin on DR 5-HT neurons may help identify candidate ion channels modulated by orexin A. To visualize and confirm the differences between the serotonergic neurons and Purkinje neurons, a tSNE plot was generated from the analysis of 64 cells and 30,244 genes (**Figure 4**). The two clusters of cells could clearly be visualized, differentiating between serotonergic neurons and Purkinje neurons. There was one DR cell among the Purkinje cells, which could be due to an error in the scRNA-seq or the normalization, but it cannot be said with certainty with this information.

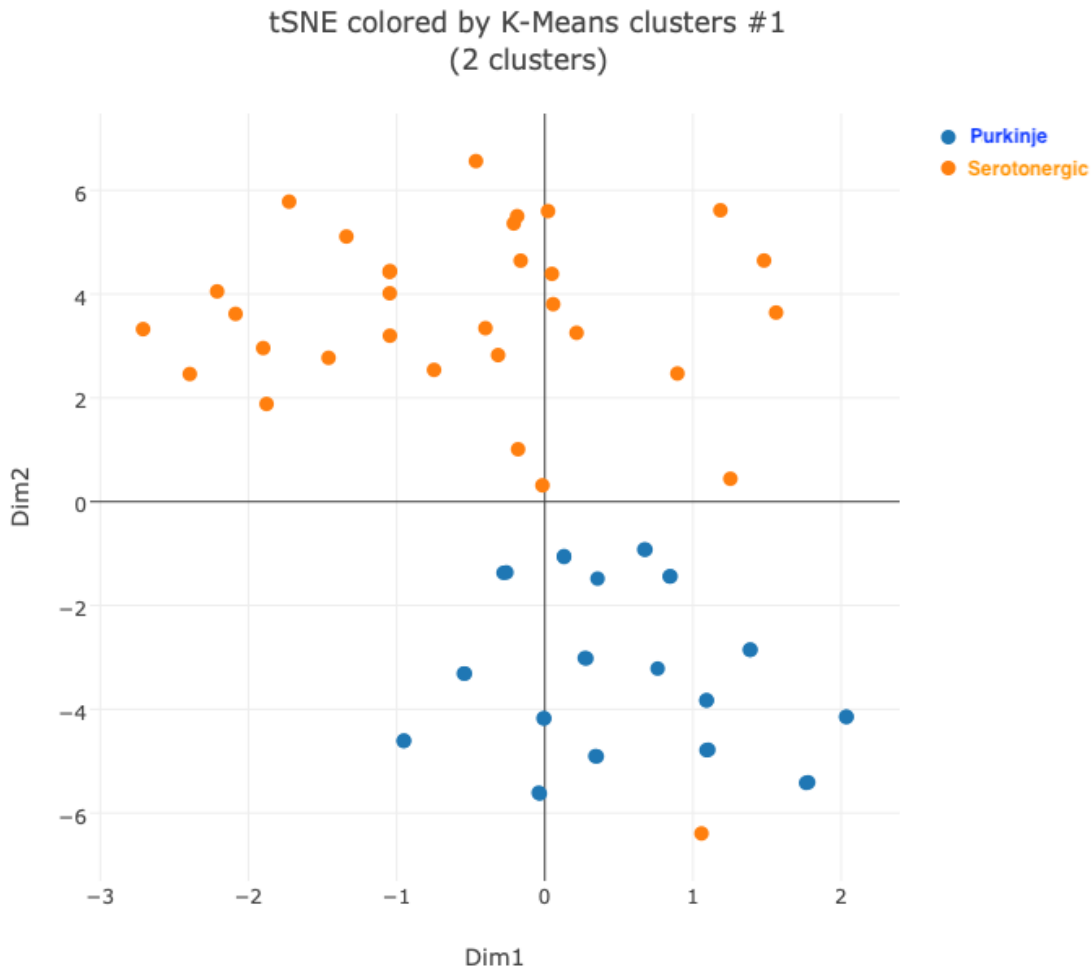


**Figure 4 | Cell cluster formation.**
tSNE plot generated from the analysis of 62 cells and 30,244 genes, using k-means clustering on normalized data with a perplexity of 21 and theta of 0.5.

Afterwards several functional gene groups were formed for the analysis of their relative gene expression profiles. These different groups of channel and receptor genes were constructed using the Amigo2 GO database with specific filters for novel orexin actions. For the calcium channels, the filters used were ion channels, neurons, GPCR and calcium. This gave us a list of 23 genes which were examined using scRNA-seq expression data.

The data was then filtered with TPM and normalized with log 2 expression for each group of genes. A heat map was generated to visualize the overall gene expression of both serotonergic and Purkinje neurons. Then, statistical analysis was done to determine the statistical significance of certain upregulated and downregulated genes.

**D.2 Analysis of calcium channel genes**

A list of calcium channel gene subunits was constructed using Amigo2 and the corresponding expression profiles were analyzed and compared between serotonergic neurons and Purkinje neurons. The difference between the dorsal and median raphe can be seen by the hierarchical clustering in the top of the heat map (**Figure 5**). The heat map shows the absolute levels of expression of the Purkinje neurons and serotonergic neurons. The heat map (**Figure 5**) also shows that eight genes have similar expression between the serotonergic and Purkinje neurons. It shows that at least 14 genes have higher gene expression in serotonergic neurons, whose statistical significance ($p$-value $< 0.05$) is confirmed (**Table 1**). The green labels indicate genes upregulated in serotonergic neurons and the red labels indicate downregulated.

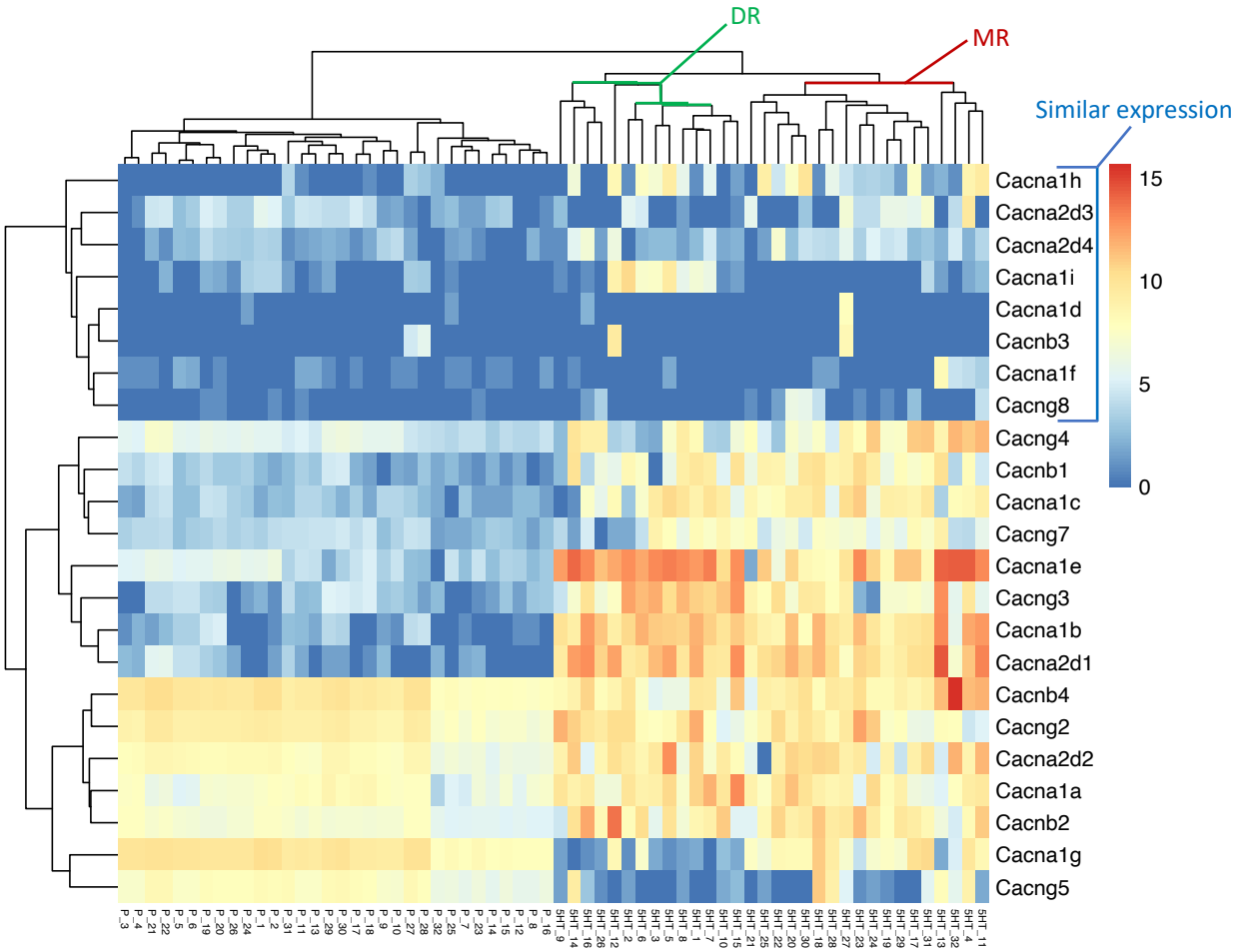


**Figure 5 | Heat map of calcium channel genes**
Showing gene expression of individual cells of both serotonergic neurons (right) and Purkinje neurons (left) with hierarchical clustering of the neurons (top) and channels genes (left).

| Gene Name | log (Fold change) | p-value | FDR |
|---|---|---|---|
| Cacna2d1 | 9.02 | 7.19e-33 | 8.26e-32 |
| Cacna1b | 8.66 | 6.41e-33 | 8.26e-32 |
| Cacna1e | 6.96 | 9.99e-21 | 7.65e-20 |
| Cacng3 | 5.92 | 3.69e-16 | 2.12e-15 |
| Cacna1c | 4.99 | 3.56e-15 | 1.63e-14 |
| Cacnb1 | 4.82 | 7.10e-15 | 2.72e-14 |
| Cacna1h | 3.90 | 1.18e-08 | 3.38e-08 |
| Cacng7 | 2.39 | 5.87e-07 | 1.35e-06 |
| Cacnb2 | 2.22 | 1.41e-06 | 2.94e-06 |
| Cacng4 | 2.01 | 0.00041 | 0.00067 |
| Cacna1a | 1.91 | 8.52e-06 | 1.63e-05 |
| Cacna2d4 | 1.52 | 0.00040 | 0.00067 |
| Cacna1i | 1.45 | 0.022 | 0.031 |
| Cacna2d2 | 1.05 | 0.036 | 0.049 |
| Cacng5 | -4.77 | 8.25e-12 | 2.71e-11 |
| Cacna1g | -3.97 | 1.53e-08 | 3.91e-08 |

**Table 1 | Differential expression of calcium channel genes**
Log2 (fold change) and p-value calculated to show statistical significance of upregulated (green) and downregulated genes (red). False discovery rate (FDR) calculated for any type 1 errors. A log2 value of 1 equals a 2-fold change (log base 2 scale).

The channels Cacna2d1 and Cacna1c from the upregulated genes (**Table 1**) are of interest because they are L-type voltage gated calcium channels (VGCCs). Orexin is known to augment Ca influx through L-type Ca2+ channels in the DR and other neurons (Kohlmeier et al., 2008). Another gene of interest is *Cacng3*, which is a VGCC. The protein encoded by *Cacng3* is a type I transmembrane AMPA receptor regulatory protein (TARP). TARPs are known to regulate both trafficking and channel gating of the AMPA receptors. The next gene of interest is *Cacnb1*, which is known to regulate the activity of L-type calcium channels that contain Cacna1a. Genes *Cacna2d1*, *Cacna1c*, and *Cacna1a* are known to show behavioral/neurological and homeostasis phenotypes (**See Appendix Table 1**), and *Cacng3* also shows homeostasis phenotypes. The phenotype information for these genes was obtained in Ensembl.

### D.3 Analysis of Glutamate receptor genes

The heat map (**Figure 6**) shows at least 9 genes that have higher expression in serotonergic neurons and at least 9 genes with higher expression in Purkinje neurons, which is confirmed by the differential expression (**Table 2**). From the list of upregulated glutamate genes (**Table 2**), the ionotropic and metabotropic glutamate receptors with a direct phenotype in nervous system, were isolated as potential candidate channels (**see Appendix Table 2)**), because agonists of glutamate receptors are known to activate orexin neurons (Li et al., 2002; Yamanaka et al., 2003).

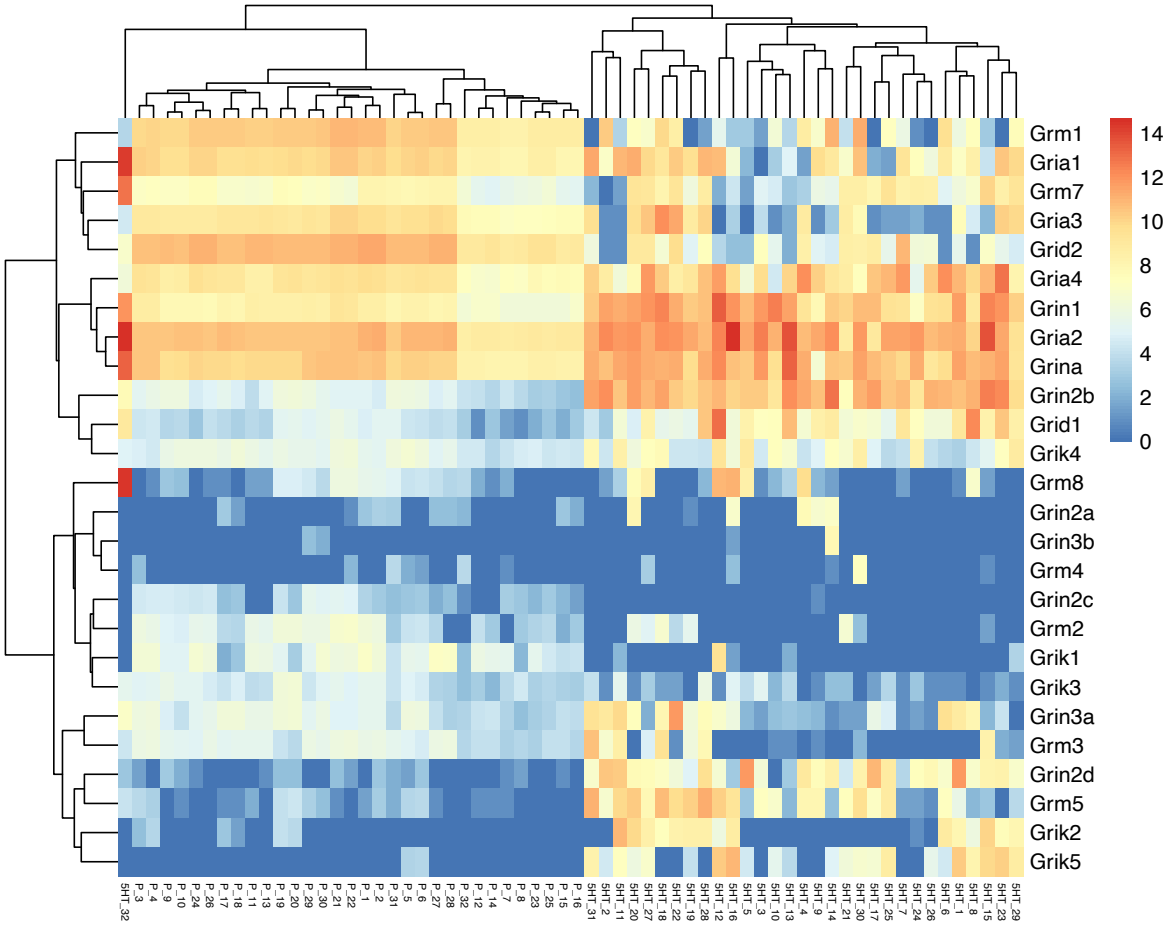


**Figure 6 | Heat map of glutamate receptor genes**
Showing gene expression of individual cells of both serotonergic neurons (right) and purkinje neurons (left) with hierarchical clustering of the neurons (top) and channels (left).

| Gene Name | log (Fold change) | p-value | FDR |
|---|---|---|---|
| Grin2d | 6.22 | 1.37e-18 | 1.78e-17 |
| Grin2b | 5.92 | 3.15e-30 | 8.19e-29 |
| Grin1 | 2.93 | 3.75e-14 | 1.95e-13 |
| Grid1 | 3.81 | 6.67e-12 | 2.48e-11 |
| Grm5 | 5.09 | 5.25e-11 | 1.71e-10 |
| Grik5 | 4.85 | 4.55e-10 | 1.18e-09 |
| Gria2 | 1.43 | 6.17e-06 | 1.14e-05 |
| Grik2 | 3.35 | 4.69e-05 | 8.13e-05 |
| Grina | 1.20 | 6.47e-05 | 0.00011 |
| Grm1 | -4.75 | 1.89e-10 | 5.45e-10 |
| Grid2 | -4.70 | 1.0061e-13 | 4.36e-13 |
| Grik1 | -4.60 | 3.50e-17 | 3.036e-16 |
| Gria3 | -3.78 | 1.79e-06 | 3.59e-06 |
| Grm2 | -3.13 | 5.20e-08 | 1.23e-07 |
| Grin2c | -2.95 | 5.179e-15 | 3.37e-14 |
| Grm3 | -2.53 | 0.00010 | 0.00015 |
| Grik3 | -2.17 | 1.039e-07 | 2.25e-07 |
| Gria1 | -1.78 | 0.0064 | 0.0092 |

**Table 2 | Differential expression of glutamate receptor genes**
Log and p-value calculated to show statistical significance of upregulated (green) and downregulated genes (red). False discovery rate (FDR) calculated for any type 1 errors. A log value of 1 equals a 2-fold change (log base 2 scale).

### D.4 Analysis of histamine, IP3, ryanodine, and orexin receptor genes

The heat map (**Figure 7**) shows 4 upregulated and 3 downregulated genes in serotonergic neurons, which is shown to be statistically significant (**Table 3**). Hierarchical clustering (**Figure 7**) also shows a connection between Hcrtr1, Hcrtr2, Hrh1 and Ryr2.

The upregulated expression of ryanodine receptor 2 (Ryr2) in the DR supports the finding of Ryanodine receptor involvement in the oeAHP (Ishibashi et al., 2016). The extremely low Hcrtr1 and Hcrtr2 expression in Purkinje cells fits with the lack of data in response of Purkinje cells to orexin and the lack of IP3 receptor expression in serotonergic neurons fits the inability to generate IP3 uncaging in dorsal raphe neurons (Ishibashi et al., 2016).

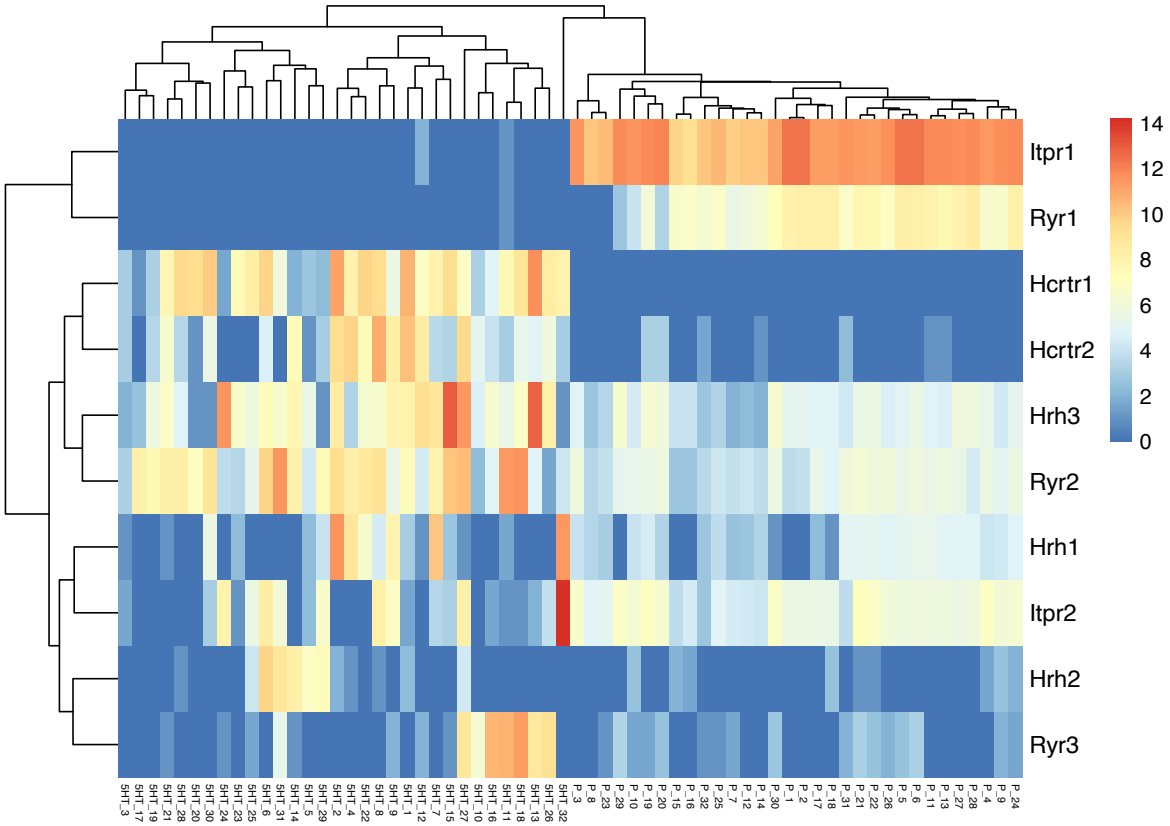


**Figure 7 | Heat map of histamine, IP3, ryanodine, and orexin receptor genes**
Showing gene expression of individual cells of both serotonergic neurons (left) and Purkinje neurons (right) with hierarchical clustering of the neurons (top) and receptor genes (left).

| Gene Name | log (fold change) | p-value | FDR |
|---|---|---|---|
| Hcrtr1 | 6.95 | 1.41e-19 | 4.69e-19 |
| Hcrtr2 | 4.31 | 9.36e-10 | 2.34e-09 |
| Ryr2 | 2.19 | 8.38e-05 | 0.00017 |
| Hrh3 | 1.75 | 0.0058 | 0.0083 |
| Hrh2 | 1.25 | 0.029 | 0.036 |
| Itpr1 | -11.18 | 1.72e-57 | 1.72e-56 |
| Ryr1 | -6.17 | 1.32e-21 | 6.59e-21 |
| Itpr2 | -2.54 | 0.00023 | 0.00038 |

**Table 3 | Differential expression of histamine, IP3, ryanodine, and orexin receptor genes**
Log2 (fold change) and p-value calculated to show statistical significance of upregulated (green) and downregulated genes (red). False discovery rate (FDR) calculated for any type 1 errors. A log2 value of 1 equals a 2-fold change (log base 2 scale).

### D.5 Analysis of TRP channel genes

The heat map (**Figure 8**) shows very similar gene expression in both serotonergic and Purkinje neurons, but the differential expression (**Table 4**) shows 4 upregulated and 5 downregulated genes in serotonergic neurons. There is a discrepancy with the heat map,

where 5 of the serotonergic neurons are separated from the others. This is because the heatmap is constructed using hierarchical clustering and the TRP genes have many differences between them, like being from different sub families and having different phenotypes attributed to the gene (**see Appendix Table 4**). The hierarchical clustering (**Figure 8**) shows a connection between Trpc7 and Trpv2. It also shows a connection between Trpc4ap and Trpm7. The high expression of TRPC3 in cerebellar purkinje cells supports a study done on synaptic transmission and motor coordination. They found that TRPC3 is a new type of postsynaptic channel that mediates mGluR- dependent synaptic transmission in cerebellar purkinje cells and that it is crucial for motor coordination (Hartmann et al., 2008).

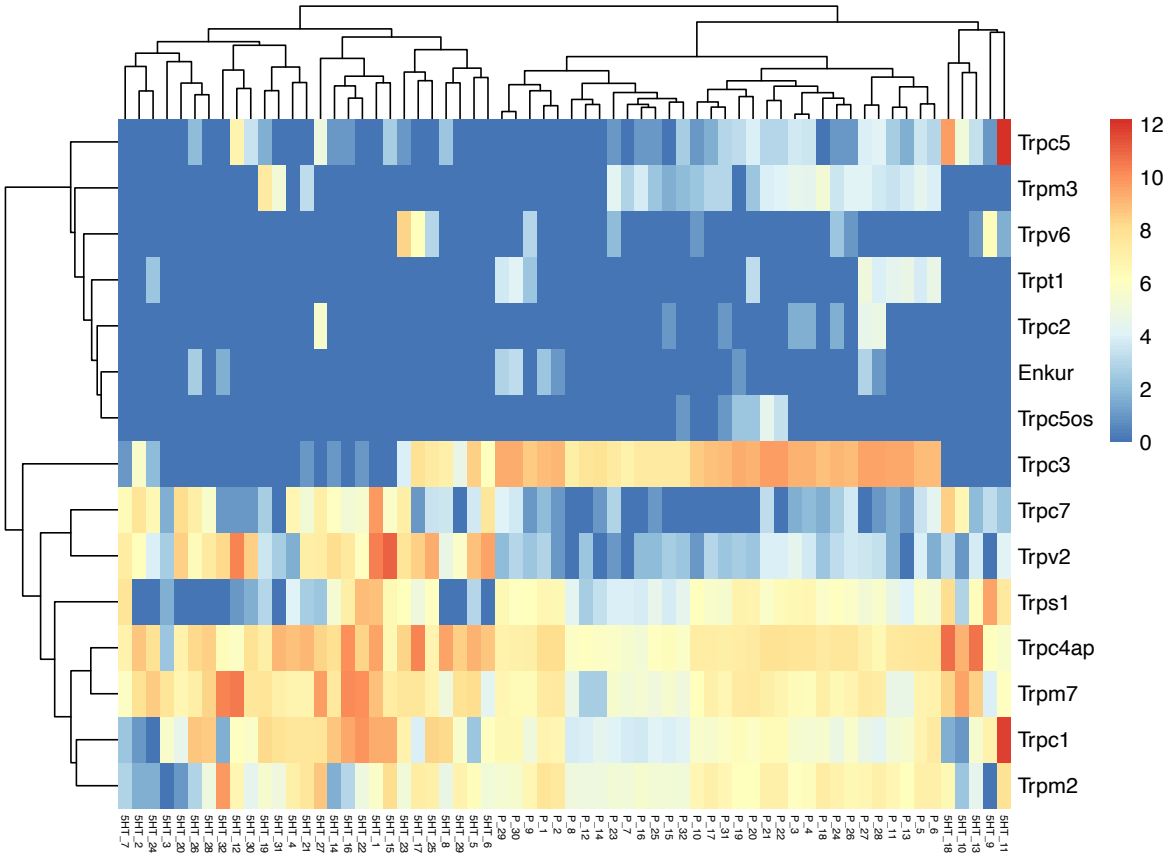


**Figure 8 | Heat map of TRP channel genes**
Showing gene expression of individual cells of both serotonergic neurons (left) and Purkinje neurons (right) with hierarchical clustering of the neurons (top) and channels (left).

| Gene Name | log (fold change) | p-value | FDR |
|---|---|---|---|
| Trpv2 | 3.97 | 6.060e-10 | 4.54e-09 |
| Trpc7 | 3.33 | 4.84e-08 | 2.42e-07 |
| Trpm7 | 1.60 | 4.23e-05 | 0.00012 |
| Trpc4ap | 1.067 | 0.0025 | 0.0054 |
| Trpc3 | -6.87 | 1.73e-20 | 2.60e-19 |
| Trpm3 | -2.036 | 1.086e-05 | 4.073e-05 |
| Trps1 | -1.76 | 0.0049 | 0.0093 |
| Trpm2 | -1.34 | 0.0061 | 0.010 |
| Trpt1 | -1.17 | 0.0013 | 0.0032 |

**Table 4 | Differential expression of TRP channel genes**
Log2 (fold change) and p-value calculated to show statistical significance of upregulated (green) and downregulated genes (red). False discovery rate (FDR) calculated for any type 1 errors. A log2 value of 1 equals a 2-fold change (log base 2 scale).

### D.6 Analysis of potassium channel genes

The heat map (**Figure 9**) shows at least 15 genes with upregulation in serotonergic neurons. Hierarchical clustering (**Figure 9**) also indicates a connection between these 4 genes. Serotonergic cell 32 is an outlier and it is unclear why it is separate from the other in the heat map. It could be that the expression of some genes in 5-HT cell 32 are more similar to some purkinje cells than they are with serotonergic neurons.

Kcnd3 is a channel of interest because it is Kv4.3 channel, which makes an A-type $K^+$ current that is inhibited by orexin (Ishibashi et al., 2016). It is shown that Kv4.3 mRNA is differentially expressed (Serôdio & Rudy, 1998), due to that, it is likely that spike broadening and increased $Ca^{2+}$ influx results from orexin mediated inhibition of A-current, mediated by Kv4.3 channels (Ishibashi et al., 2016).

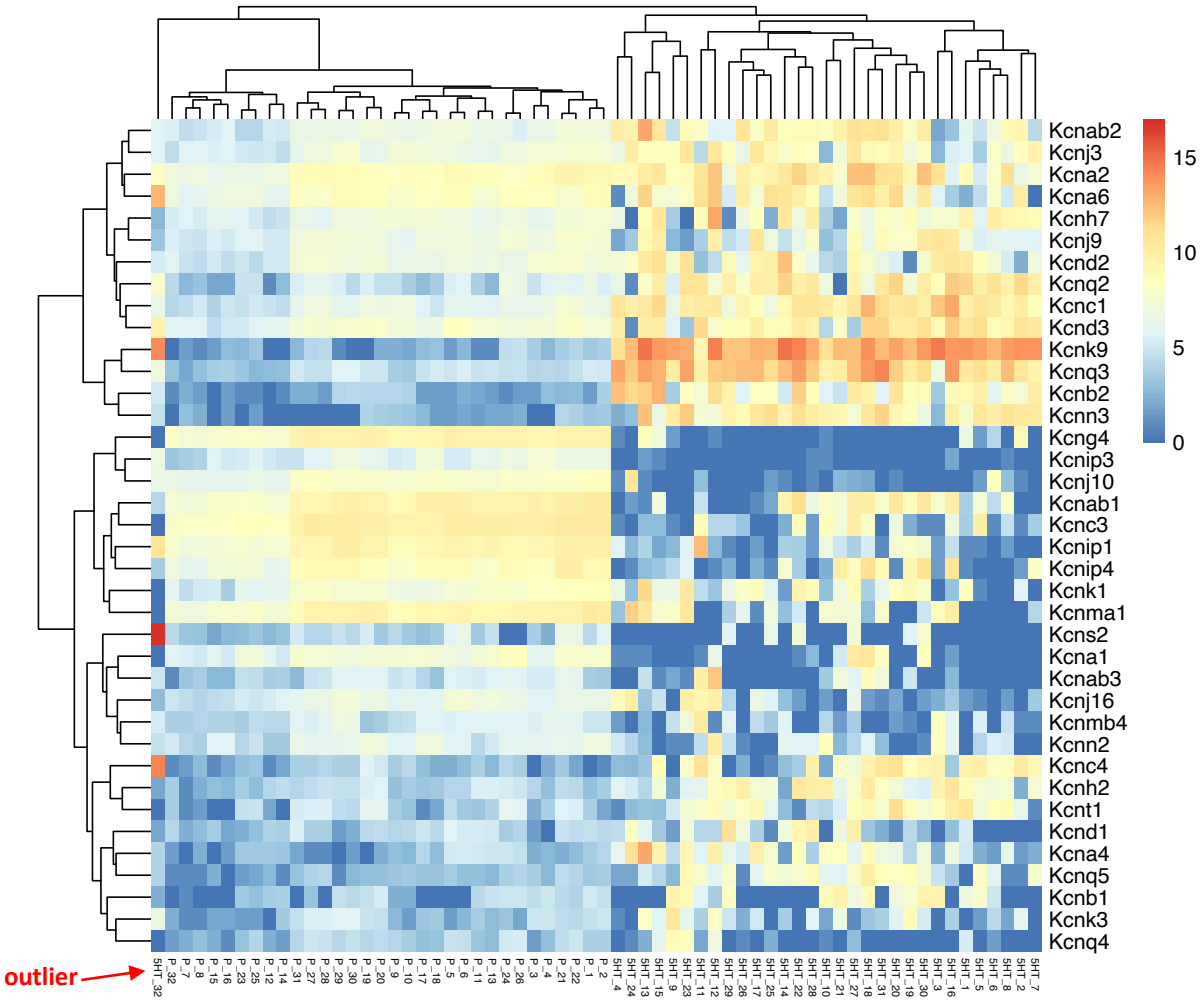


**Figure 9 | Heat map of potassium channel genes**
Showing gene expression of individual cells of both serotonergic neurons (right) and purkinje neurons (left) with hierarchical clustering of the neurons (top) and channels (left).

| Gene Name | log (fold change) | p-value | FDR |
|---|---|---|---|
| Kcnk9 | 10.78 | 5.866e-42 | 2.22e-40 |
| Kcnq3 | 7.17 | 4.88e-29 | 9.27e-28 |
| Kcnn3 | 7.16 | 1.93e-21 | 1.47e-20 |
| Kcnb2 | 6.27 | 1.065e-19 | 5.78e-19 |
| Kcnq2 | 4.32 | 3.53e-11 | 1.12e-10 |
| Kcnc1 | 3.95 | 1.20e-16 | 5.71e-16 |
| Kcnc4 | 3.89 | 6.21e-07 | 1.24e-06 |
| Kcna4 | 3.54 | 6.075e-08 | 1.44e-07 |
| Kcnh2 | 3.05 | 2.19e-08 | 5.57e-08 |
| Kcnq5 | 2.99 | 3.91e-07 | 8.750e-07 |
| Kcnt1 | 2.72 | 4.97e-05 | 9.0018e-05 |
| Kcnab2 | 1.96 | 0.00014 | 0.00022 |
| Kcnd3 | 1.94 | 0.00025 | 0.00037 |
| Kcna2 | 1.33 | 0.0014 | 0.0019 |
| Kcnj3 | 1.12 | 0.014 | 0.017 |
| Kcng4 | -7.69 | 1.43e-24 | 1.36e-23 |
| Kcnj10 | -6.025 | 7.67e-20 | 4.86e-19 |
| Kcnc3 | -5.79 | 1.15e-14 | 4.87e-14 |
| Kcnip3 | -5.48 | 1.026e-25 | 1.30e-24 |
| Kcnip1 | -5.25 | 1.65e-13 | 6.28e-13 |
| Kcna1 | -5.19 | 4.84e-13 | 1.67e-12 |
| Kcnma1 | -4.51 | 9.0054e-09 | 2.63e-08 |
| Kcnip4 | -4.35 | 1.62e-08 | 4.40e-08 |
| Kcnab1 | -3.94 | 4.36e-07 | 9.21e-07 |
| Kcnj16 | -2.75 | 1.38e-05 | 2.62e-05 |
| Kcnn2 | -2.28 | 7.63e-05 | 0.00013 |
| Kcnmb4 | -2.23 | 9.11e-05 | 0.00015 |
| Kcnab3 | -2.22 | 0.00088 | 0.0012 |
| Kcns2 | -2.040 | 0.0054 | 0.0071 |
| Kcnq4 | -2.038 | 0.00017 | 0.00026 |
| Kcnk1 | -1.62 | 0.012 | 0.015 |

**Table 5 | Differential expression of potassium channel genes**
Log2(fold change) and p-value calculated to show statistical significance of upregulated (green) and downregulated genes (red). False discovery rate (FDR) calculated for any type 1 errors. A log2 value of 1 equals a 2-fold change (log base 2 scale).

### D.7 Analysis of Na, K, Ca-dependent, and non-voltage gated ion channel genes

There are nearly 25 genes that show upregulation in serotonergic neurons (**Figure 10**). All of these genes are statistically significant as shown in the differential expression (**Table 6**).

The upregulated solute carrier genes in this group could be potential candidate genes. Slc6a4 is a 5-HT neurotransmitter transporter that is highly expressed in serotonergic neurons and absent in Purkinje cells. Another gene of interest is Slc22a17,

which is a cell surface receptor for lipocalin2 (LCN2) that plays a key role in iron homeostasis and transport. It is able to bind iron bound LCN2 (holo-24p3), followed by internalization of holo-24p3 and release of iron, thereby increasing intracellular iron concentration and leading to inhibition of apoptosis (Bennett et al., 2011). Another possible candidate is Slc35a22, which is involved in the transport of glutamate (with $H^+$) across the inner mitochondrial membrane (Goubert et al., 2017).

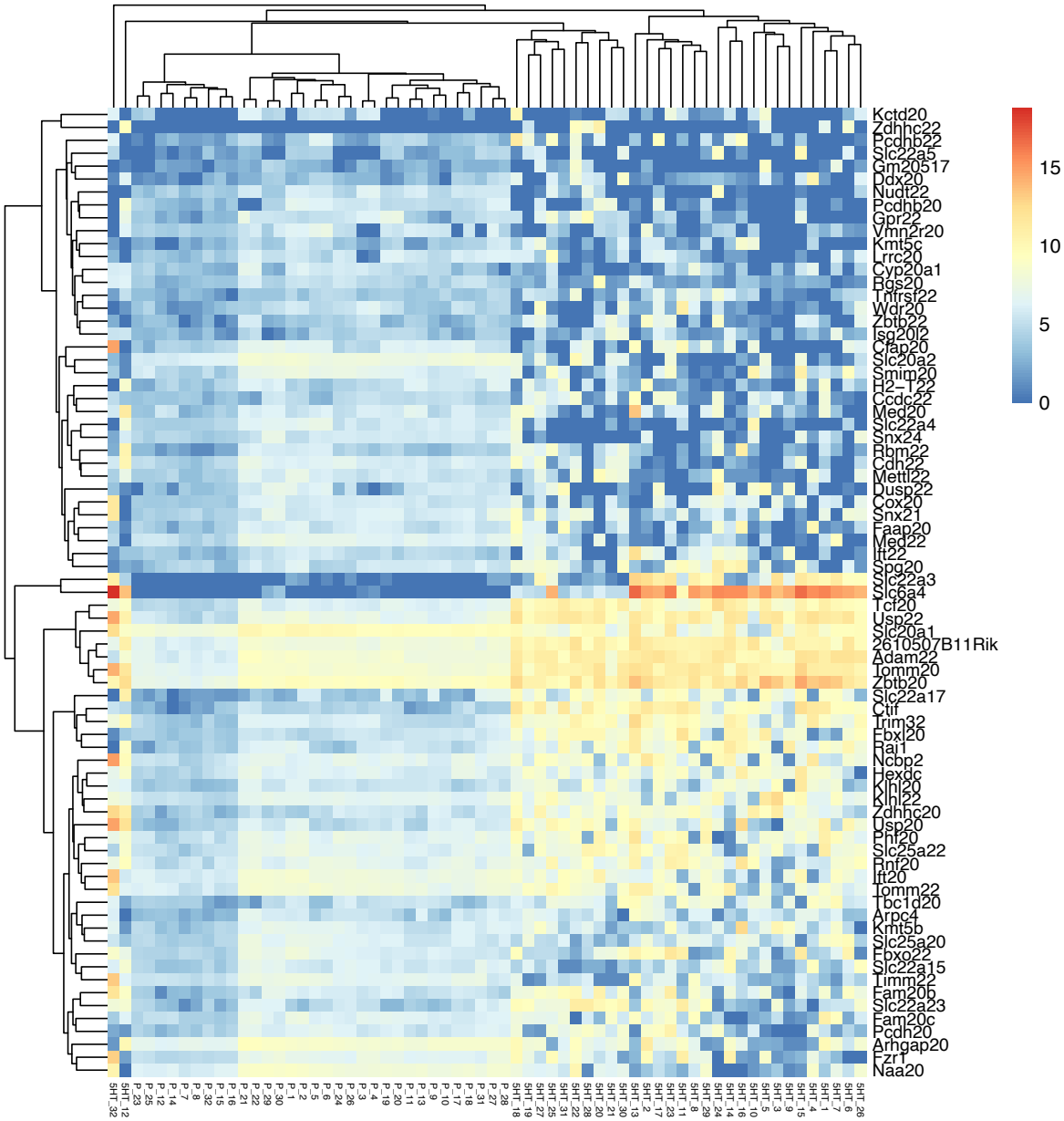


**Figure 10 | Heat map of Na, K, Ca-dependent, and non-voltage gated ion channel genes**
Showing gene expression of individual cells of both serotonergic neurons (right-left) and Purkinje neurons (middle) with hierarchical clustering of the neurons (top) and ion channels (left).

| Gene Name | log (fold change) | p-value | FDR |
|---|---|---|---|
| Slc6a4 | 11.88 | 1.37e-23 | 1.028e-21 |
| Slc22a3 | 6.75 | 8.65e-14 | 8.0065e-13 |
| Ctif | 5.61 | 1.028e-18 | 3.80e-17 |
| Usp22 | 4.23 | 6.26e-18 | 1.54e-16 |
| Tcf20 | 3.92 | 2.25e-19 | 1.67e-17 |
| Slc22a17 | 3.70 | 1.018e-08 | 5.38e-08 |
| Trim32 | 3.65 | 2.20e-14 | 2.71e-13 |
| Zdhhc20 | 3.21 | 1.21e-10 | 7.47e-10 |
| Zbtb20 | 3.14 | 6.73e-14 | 7.12e-13 |
| Tomm20 | 3.12 | 7.20e-16 | 1.33e-14 |
| 2610507B11Rik | 2.91 | 9.71e-15 | 1.43e-13 |
| Adam22 | 2.90 | 8.56e-12 | 7.038e-11 |
| Rai1 | 2.89 | 6.016e-07 | 2.782e-06 |
| Usp20 | 2.89 | 4.86e-06 | 1.79e-05 |
| Fbxl20 | 2.76 | 3.58e-06 | 1.39e-05 |
| Slc22a23 | 2.41 | 0.00018 | 0.00056 |
| Tbc1d20 | 2.14 | 2.23e-05 | 7.51e-05 |
| Zdhhc22 | 2.067 | 0.00154 | 0.0033 |
| Fam20b | 1.97 | 0.00073 | 0.0017 |
| Klhl20 | 1.73 | 0.00025 | 0.00076 |
| Hexdc | 1.53 | 0.00065 | 0.0016 |
| Klhl22 | 1.49 | 0.00051 | 0.0013 |
| Ncbp2 | 1.43 | 0.010 | 0.017 |
| Rnf20 | 1.33 | 0.0032 | 0.0064 |
| Slc25a22 | 1.25 | 0.014 | 0.024 |
| Phf20 | 1.16 | 0.030 | 0.049 |
| Slc20a2 | -4.36 | 2.15e-10 | 1.22e-09 |
| Slc22a4 | -3.99 | 9.30e-11 | 6.26e-10 |
| Nudt22 | -3.62 | 7.97e-11 | 5.90e-10 |
| Snx24 | -3.15 | 2.0061e-07 | 9.89e-07 |
| Med22 | -2.95 | 7.51e-07 | 3.27e-06 |
| Naa20 | -2.94 | 2.013e-06 | 8.27e-06 |
| Pcdhb20 | -2.66 | 1.29e-05 | 4.57e-05 |
| Vmn2r20 | -2.23 | 9.80e-05 | 0.00031 |
| Cdh22 | -2.22 | 0.00032 | 0.00092 |
| Smim20 | -2.15 | 0.00081 | 0.0018 |
| Arhgap20 | -2.021 | 0.00077 | 0.0017 |
| Lrrc20 | -1.96 | 0.00066 | 0.0016 |
| Cfap20 | -1.83 | 0.012 | 0.022 |
| Mettl22 | -1.77 | 0.0037 | 0.0073 |
| Wdr20 | -1.68 | 0.0046 | 0.0088 |
| Timm22 | -1.65 | 0.0020 | 0.0043 |
| Gpr22 | -1.65 | 0.0081 | 0.014 |
| Cyp20a1 | -1.63 | 0.0022 | 0.0045 |
| H2-T22 | -1.56 | 0.0076 | 0.014 |
| Rgs20 | -1.51 | 0.00050 | 0.0013 |
| Faap20 | -1.38 | 0.022 | 0.037 |

**Table 6 | Differential expression of Na, K, Ca-dependent, and non-voltage gated ion channel genes – showing statistical significance**

### D.8 Analysis of Na or Ca-dependent, non-voltage gated ion channels

The heatmap (**Figure 11**) and the differential expression (**Table 7**) show 20 genes that are upregulated in serotonergic neurons and 11 genes that are downregulated. The hierarchical clustering (**Figure 11**) shows a connection between Nalcn and Trpm7, Grin2b, and Slc1a4. Hcn3 is a potential candidate because it is a hyperpolarization activated potassium channel. It may also facilitate the permeation of sodium ions. It is also inhibited by cesium (Negrini et al., 2016) and ZD7288 (Wu et al., 2012).

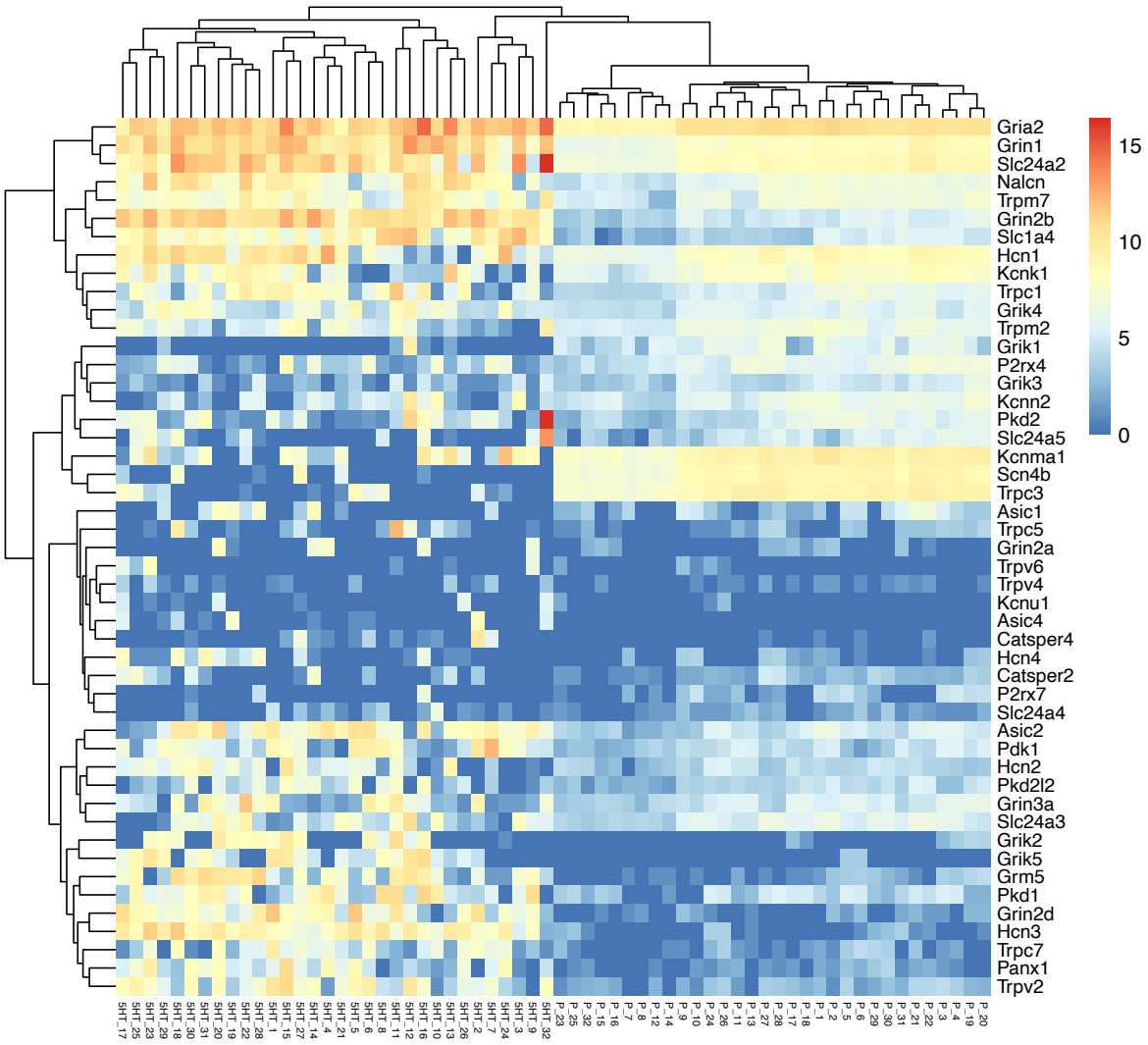


**Figure 11 | Heat map of Na or Ca-dependent non-voltage gated ion channels.**
Showing gene expression of individual cells of both serotonergic neurons (left) and Purkinje neurons (right) with hierarchical clustering of the neurons (top) and ion channels (left).

| Gene Name | log (fold change) | p-value | FDR |
|---|---|---|---|
| Hcn3 | 7.63 | 7.88e-29 | 1.89e-27 |
| Grin2d | 6.21 | 5.87e-19 | 5.64e-18 |
| Grin2b | 5.91 | 1.096e-29 | 5.26e-28 |
| Grm5 | 5.091 | 2.74e-11 | 1.46e-10 |
| Grik5 | 4.85 | 2.51e-10 | 1.20e-09 |
| Slc1a4 | 4.75 | 8.25e-17 | 5.65e-16 |
| Trpv2 | 3.97 | 4.70e-10 | 1.88e-09 |
| Panx1 | 3.93 | 4.52e-10 | 1.88e-09 |
| Grik2 | 3.35 | 3.51e-05 | 7.66e-05 |
| Trpc7 | 3.33 | 4.24e-08 | 1.45e-07 |
| Asic2 | 2.95 | 1.27e-06 | 3.81e-06 |
| Pkd1 | 2.94 | 2.30e-05 | 5.52e-05 |
| Grin1 | 2.93 | 1.48e-13 | 8.89e-13 |
| Nalcn | 2.38 | 1.79e-06 | 5.078e-06 |
| Slc24a2 | 2.22 | 7.20e-06 | 1.92e-05 |
| Pdk1 | 1.78 | 0.0025 | 0.0045 |
| Trpm7 | 1.60 | 7.060e-05 | 0.00014 |
| Gria2 | 1.43 | 1.52e-05 | 3.85e-05 |
| Asic4 | 1.14 | 0.0090 | 0.015 |
| Catsper4 | 1.031 | 0.018 | 0.028 |
| Scn4b | -7.51 | 5.37e-27 | 8.59e-26 |
| Trpc3 | -6.87 | 7.10e-21 | 8.52e-20 |
| Grik1 | -4.60 | 3.49e-17 | 2.79e-16 |
| Kcnma1 | -4.51 | 1.066e-08 | 3.93e-08 |
| Kcnn2 | -2.28 | 6.77e-05 | 0.00014 |
| Grik3 | -2.17 | 1.71e-07 | 5.48e-07 |
| P2rx4 | -2.11 | 3.42e-05 | 7.66e-05 |
| Slc24a5 | -2.096 | 0.0022 | 0.0040 |
| Kcnk1 | -1.62 | 0.012 | 0.019 |
| P2rx7 | -1.54 | 0.00047 | 0.00091 |
| Trpm2 | -1.34 | 0.0066 | 0.011 |

**Table 7 | Differential expression of Na or Ca-dependent non-voltage gated ion channel genes.** Log2 (fold change) and p-value calculated to show statistical significance of upregulated (green) and downregulated genes (red). False discovery rate (FDR) calculated for any type 1 errors. A log2 value of 1 equals a 2-fold change (log base 2 scale).

### D.9 Analysis of potential candidate genes

After the breakdown and analysis of multiple groups of genes, we isolated potential genes that were highly expressed in serotonergic neurons and displayed some properties that might mediate orexin neuropeptide action on serotonergic neurons. Isolating channels from each group analyzed, we compiled a group of channels to do scRNA-seq analysis on. These are potential channels that might exhibit novel effects which both excites the neurons and alters their firing pattern by lengthening the spike afterhyperpolarization

(Ishibashi et al., 2016). The goal is to find cells with high SK3 expression and cation channels that are not directly gated by ligand, but gated by second messengers, in particular protein kinase C (PKC) activation. Also, these channels should not be blocked by extracellular cesium but inhibited by extracellular and intracellular $Ca^{2+}$.

The first channel of interest is Kcnn3, which is a small-conductance calcium-activated potassium channel (SK3). A few channels who have similar expression to Kcnn3 are Cacna1a, Nalcn, Hcn3, and Trpc4ap. All these channels seem to have a similar gene expression profiles, as seen by the hierarchical clustering (**Figure 12**) of the DR and MR serotonergic neurons. Kcnn3 also shows function at the plasma membrane (**see Appendix Table 5**). It has been shown that PKC enhances plasma membrane expression of cardiac L-type calcium channels (Hofmann, 2018; Raifman et al., 2017). So, channels with function at plasma membrane and/or relation to cardiovascular system, could indicate that the channel might be activated by PKC or at least could has some relationship to PKC.

Other genes that have shown function in the plasma membrane and are related to the cardiovascular system are Cacna2d1, Cacna1b, Cacna1c (**see Appendix Table 1**), Grin2d, Grin1 (**See Appendix Table 2**), Ryr2 (**see Appendix Table 3**), Trpc6 (**see Appendix Table 4)**, Slc6a4 (**see Appendix Table 6**), Hcn3, and Asic4 (**see Appendix Table 7**). Another possibility is a combination of Trpc3, Trpc6, and Trpc7. These channels hetero-multimerize and exhibit the right properties. A concern here is that Trpc6 does not seem to show any expression in serotonergic neurons or Purkinje neurons. Ultimately, the channel chosen was Nalcn, which was differentially expressed in the serotonergic neurons and it has the possibility that it might mediate the several novel effects of orexin that have been described.

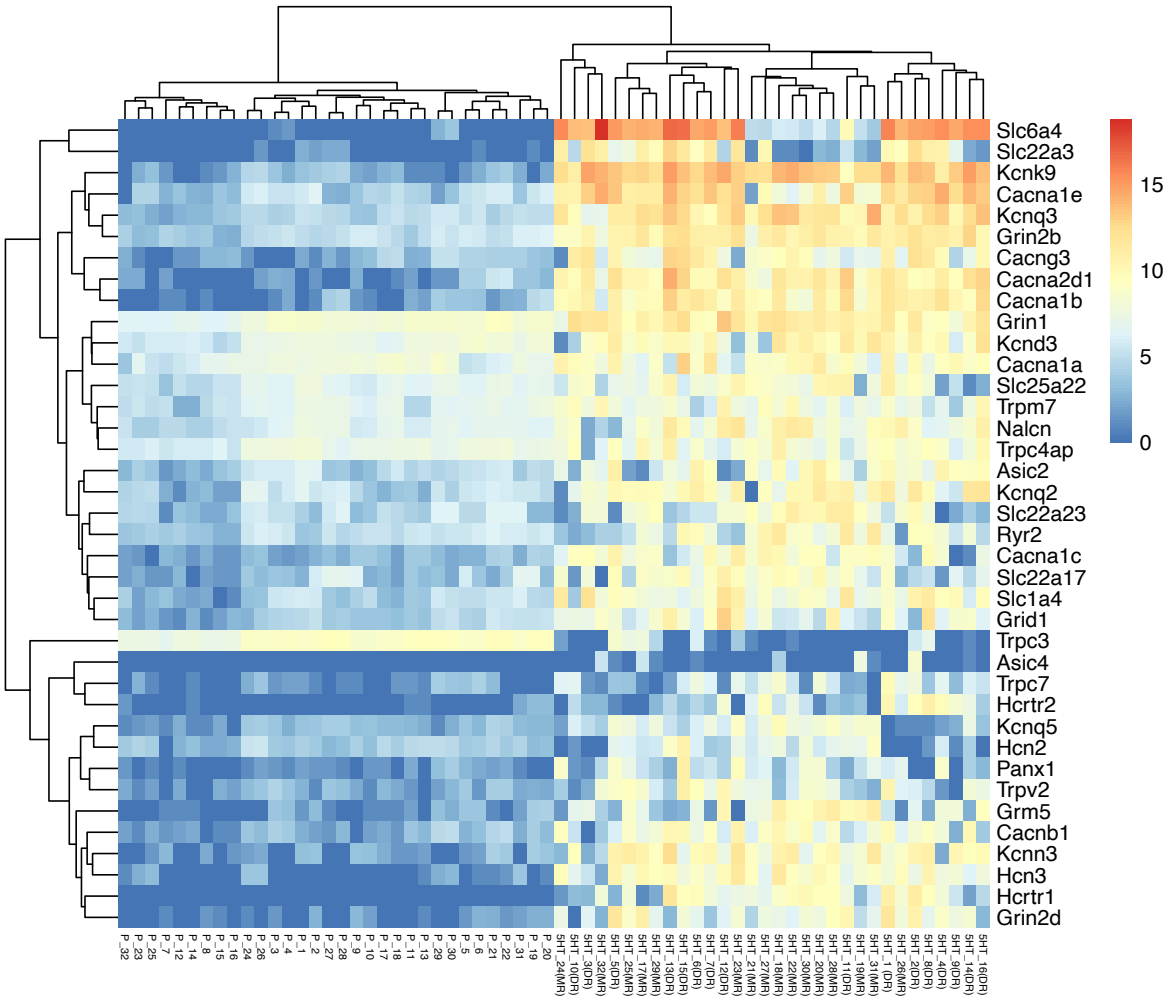


**Figure 12 | Heat map of potential candidate genes – both 5-HT and Purkinje cells**
Showing gene expression of individual cells of both serotonergic neurons (right) and Purkinje neurons (left) with hierarchical clustering of the neurons (top) and channel genes (left).

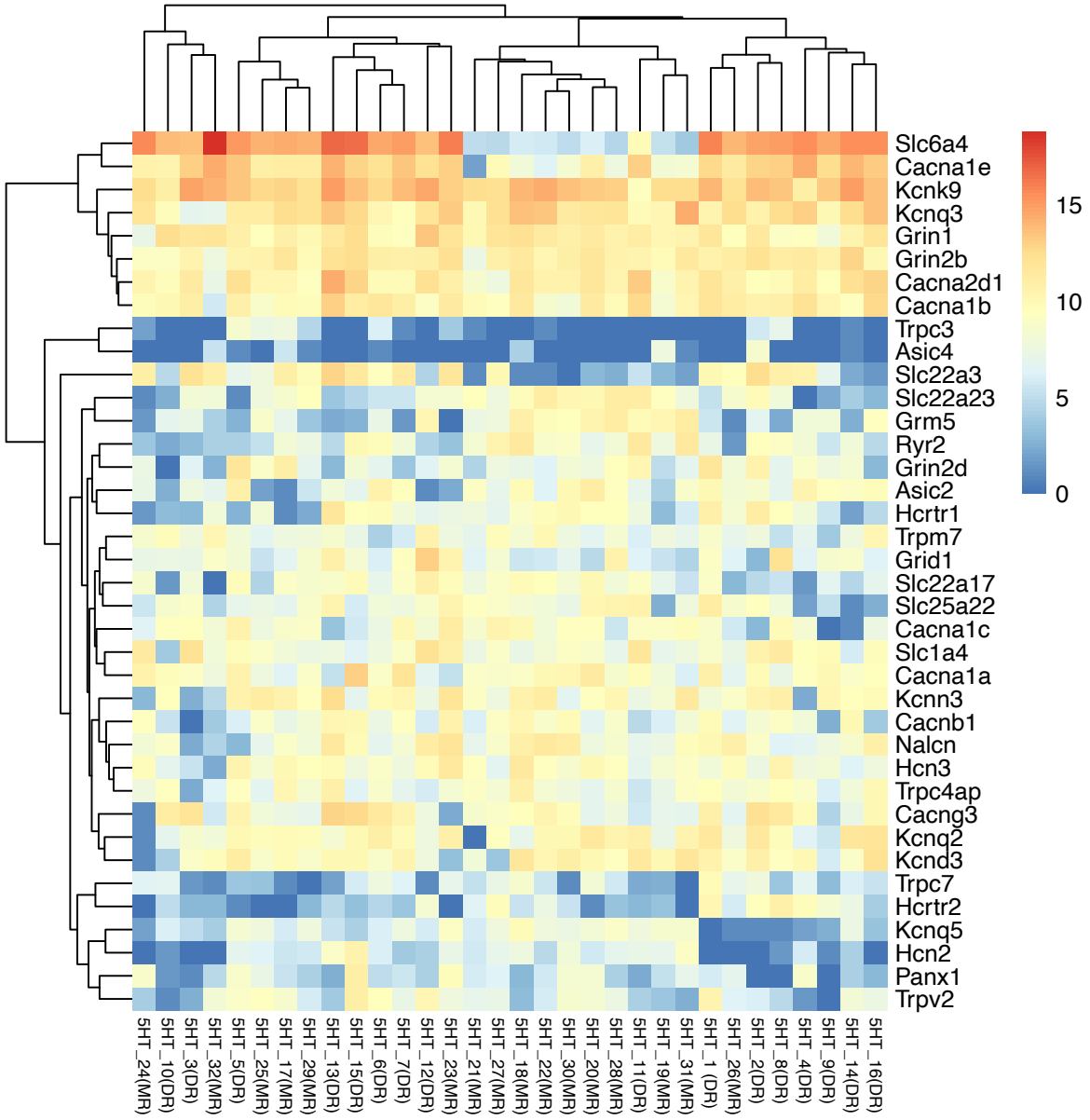


**Figure 13 | Heat map of potential candidate genes – 5-HT only**
Showing gene expression of individual cells of serotonergic neurons with hierarchical clustering of the neurons (top) and gens (left).

**Aim 2: Testing a candidate ion channel**

**D.10 Expression of Nalcn**

The list of potential channels has been narrowed down to 17 genes from a few hundred. From those 17 genes, only 7 are upregulated in Serotonergic neurons vs Purkinje cells. One of those upregulated channels in DR 5-HT neurons is Nalcn, which is a sodium leak channel that is modulated by GPCRs and also inhibited by extracellular [$Ca^{2+}$].

Our first step of testing this channel was to confirm Nalcn protein is expressed in DR 5-HT neurons. To do that, we sought to determine an effective concentration of a commercially available anti-Nalcn antibody by exploring both a highly sensitive VIP immunocytochemistry approach and an indirect immunofluorescence approach to visualize immunoreactivity. Then we used this antibody to determine whether there was Nalcn immunostaining in the DR and whether there was Nalcn present in serotonergic neurons. Since our ultimate goal is to knock out the channel to test its role in mediating orexin responses, we next wanted to confirm that we could detect Nalcn protein in the DR of mice with the Nalcn gene floxed ($Nalcn^{FL/FL}$). We first confirmed a normal expression pattern of 5-HT neurons in $Nalcn^{FL/FL}$ mice using an antibody to TPH (the rate-limiting enzyme in 5-HT biosynthesis). We then determined if Nalcn expression could be detected in these neurons. After that, our goal was to determine whether we could block Nalcn immunostaining in DR neurons by expressing Cre- recombinase in the DR delivered by microinjection of a viral vector (AAV) at different time points prior to conducting immunocytochemistry.

**D.11 Finding an effective concentration of the anti-Nalcn antibody (#ASC-022)**

VIP immunohistochemistry was selected because it is generally more sensitive than immunofluorescence and ion channels, which are low abundance proteins are very challenging to reliably visualize with immunocytochemistry. Moreover, the commercially available antibody, which was made to an extracellular domain of the channel protein, has not been published. We therefore tested different concentrations of the antibody. We tested [1:1000] (**Figure 14A**), [1:500] (**Figure 14B**) and [1:200] dilutions. Nalcn staining with these concentrations from the VIP done was not convincing since the VIP reaction required long durations and produced significant background staining that was observed in appeared cell nuclei, which are not expected to contain authentic staining. We tried to improve the VIP immunohistochemistry by using [1:200] (**Figure 14C**) with some altered conditions. Instead of 1-day incubation with the primary antibody, tissue was incubated for 2 days at 4 degrees Celsius with agitation. This was because with 1 day incubation there wasn't sufficient Nalcn staining visible. Also, the ethanol and xylene wash steps were also reduced by half, in case that was causing a reduction in staining. These changes improved the results but not by much. At last, the VIP was repeated using a higher concentration [1:100 dilution] of the primary antibody (**Figure 14D**), which improved the results, and the staining could be properly visualized with reaction product on neuronal membranes and less apparent non-specific staining of nuclei.

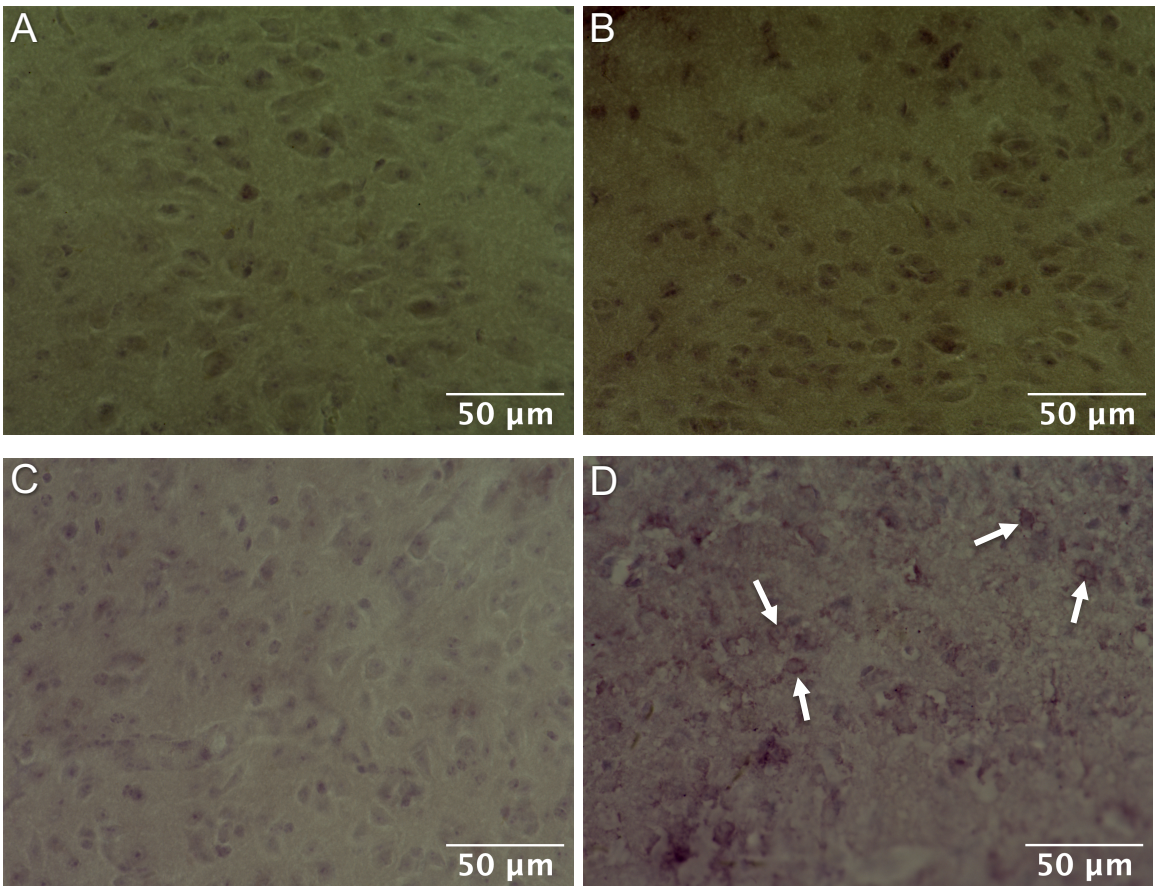


**Figure 14 | Expression of Nalcn at different concentrations of Nalcn antibody**
**(A)** VIP using [1:1000] of Nalcn antibody with an exposure time of 3.5 mins. **(B)** VIP using [1:500] of Nalcn antibody with an exposure time of 2 mins. **(C)** VIP using [1:200] of Nalcn antibody with an exposure time of 1 min. **(D)** VIP using [1:100] of Nalcn antibody with an exposure time of 1 min. This was done using VIP Immunohistochemistry with Anti Nalcn/VGCNL1 (extracellular) antibody. The white arrows are indicating the Nalcn expression due to the extracellular antibody at [1:100]. The location of these images was superior to the aqueduct. The images were taken with 60x objective. The scale bar is 50um.

### D.12 Nalcn immunostaining in TPH+ DR neurons in Sert-Cre/dTom mice

The next series of experiments we wanted to determine whether Nalcn was present in the Dorsal Raphe and whether it could be visualized in 5-HT neurons. For this we wanted to use double labelling which is generally more successful if it can be done with fluorescence tags. Surprisingly, the Nalcn immunofluorescence seemed more reliable than the VIP staining, in that the background between the cells was lower and there was little apparent nuclear staining (**Figure 15**). Success with immunofluorescence allowed us to use

Sert-Cre/dTom mice (**Figure 15**) which express bright red fluorescence selectively in 5-HT neurons in the DR (Li et al., 2016; Ren et al., 2019). By doing immunohistochemistry on Sert-Cre: dTom mice, it was confirmed that Nalcn immunostaining was present in the DR (**Figure 15**).

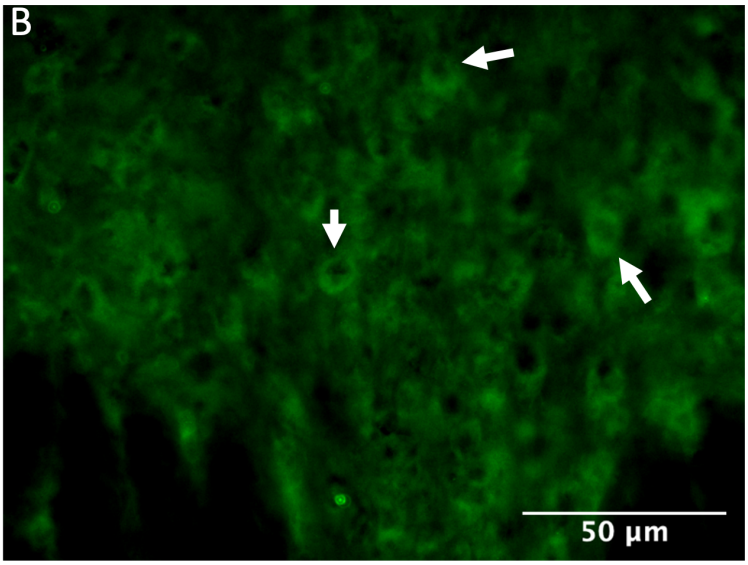


**Figure 15 | Expression of Nalcn in the DR of Sert-Cre/dTom mice.**
Expression of Nalcn in Sert-Cre/dTom mice using [1:100] Nalcn antibody and Alexa Fluor 488. These images were taken with 40x Objective.

After confirming Nalcn Immunostaining in the DR, we needed to determine if there was expression of Nalcn in serotonergic neurons. This was done using Immunohistochemistry. We did immunohistochemistry using [1:100] of Nalcn antibody and Alexa Fluor 488 on Sert-Cre/dTom mice. It was clearly visible from the superimposed image that Nalcn immunostaining is present in dTom fluorescent neurons (**Figure 16C**). It is also apparent from this image that some Nalcn immunopositive neurons are not dTom positive (**Figure 16 open arrows**), suggesting that some non-serotonergic neurons also express Nalcn protein.

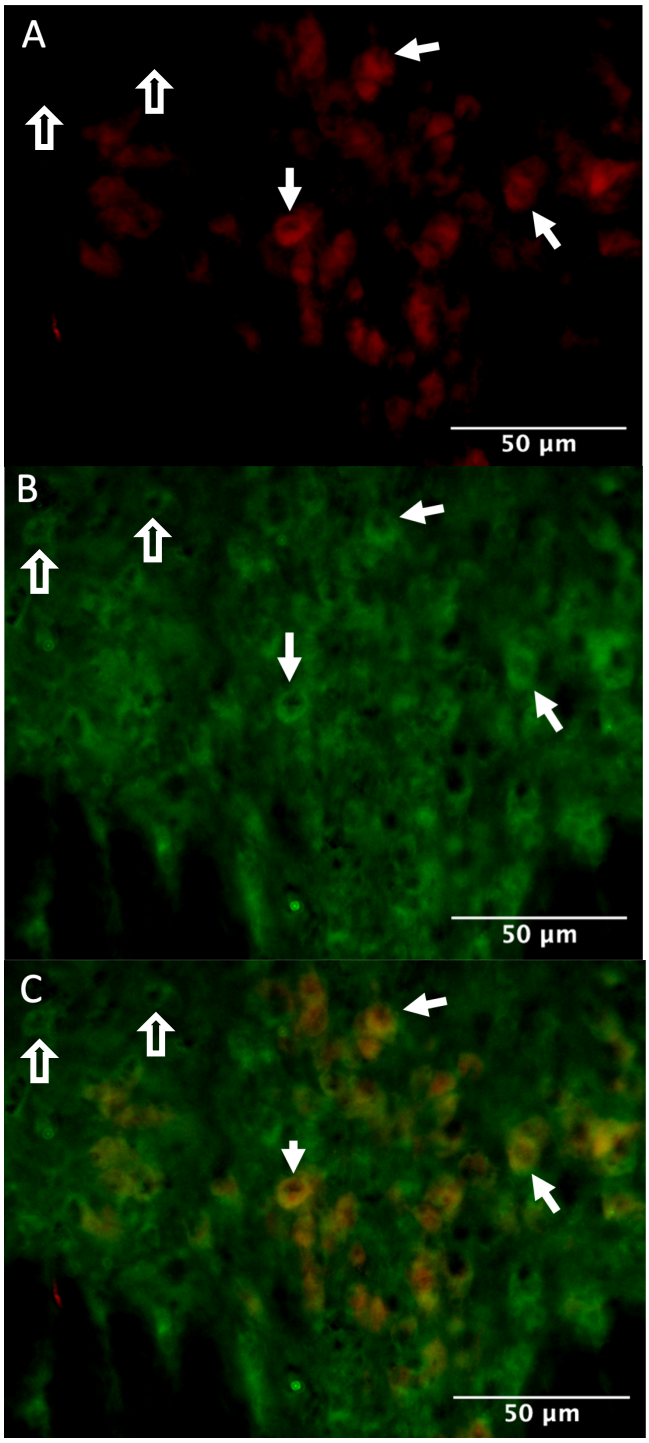


**Figure 16 | Expression of Nalcn in Serotonergic Neurons of the DR**
**(A)** Expression of serotonergic neurons in the DR of a Sert Tom + mouse. **(B)** Expression of Nalcn in the DR of a Sert Tom + mouse. **(C)** Overlap of the expression of serotonergic neurons and Nalcn. These images were taken using a 40x objective. Open arrows show Nalcn immunopositive neurons are not dTom positive.

### D.13 Expression of TPH in the Nalcn$^{FL/FL}$ mice

Since we were using NalcnFL/FL mice, it was important to determine that we could detect Nalcn in the DR of these mice and that there was normal expression of serotonergic neurons in the Dorsal raphe of these mice. Immunostaining in the Nalcn$^{FL/FL}$ mice (**Figure 17**) showed that we could still detect Nalcn immunofluorescence in these engineered mice. Nevertheless, our subjective impression was that cellular definition was less clear in sections from these mice, although the reason for this is not clear. To confirm that 5-HT neurons were normally distributed in these mice we used anti-Tph as the primary antibody and Alexa Fluor 594 was used as the secondary antibody. The TPH immunofluorescence in the Nalcn$^{FL/FL}$ (**Figure 18A**) was compared with that in C57Blk6 mice (**Figure 18B**). It was clear by the immunohistochemistry results that TPH+ neurons in Nalcn$^{FL/FL}$ mice had shapes and distributions that were qualitatively similar to what we observed in the C57Blk6 mice.

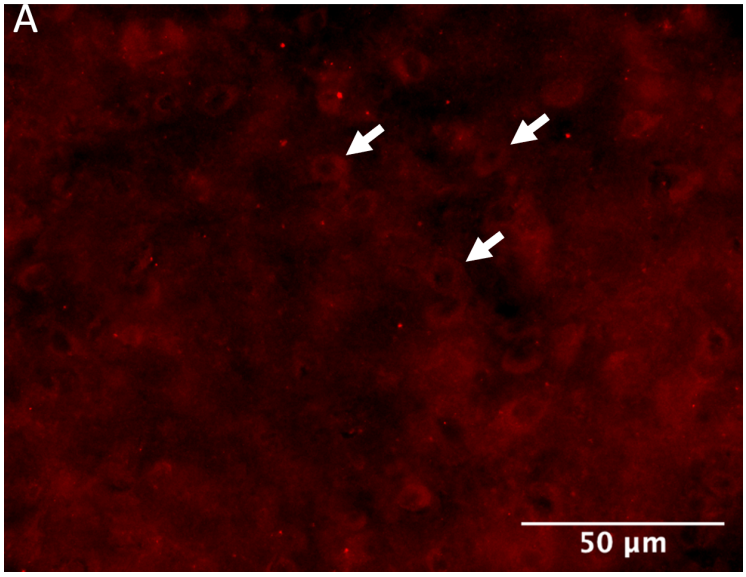


**Figure 17 | Expression of Nalcn in the DR of Nalcn$^{FL/FL}$**
Expression of Nalcn in Nalcn$^{FL/FL}$ mice using Nalcn antibody and Alexa Fluor 594.

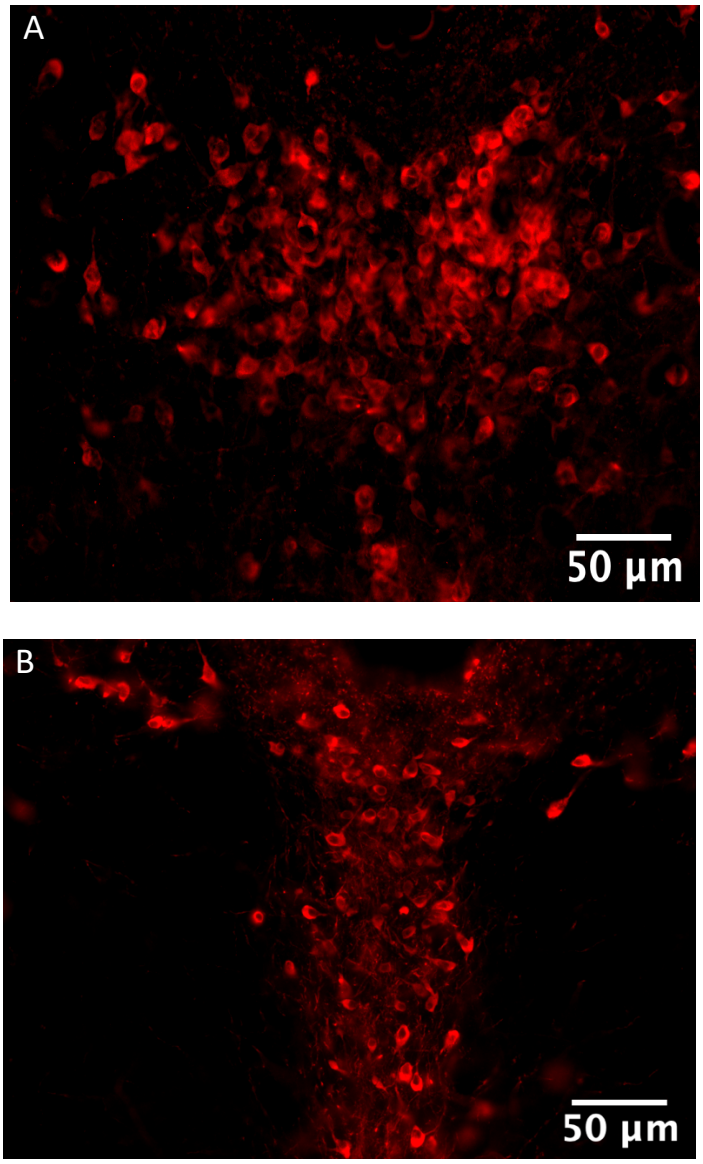


**Figure 18 | Serotonergic Neurons in Nalcn$^{FL/FL}$ and wildtype C57Blk6 appeared similar in shape and distribution.**
**(A)** Expression of Serotonergic Neurons in the DR of Nalcn$^{FL/FL}$. **(B)** Expression of Serotonergic Neurons in the DR of Blk6. These images were taken using a 20x objective.

### D.14 Determining if Cre expression blocks Nalcn immunostaining

The next goal was to reduce or knock out the expression of Nalcn from the DR. The Nalcn$^{FL/FL}$ mice used were from the Jackson laboratory, in which Exons 5 and 6 of the mouse Nalcn gene are flanked by the loxP sites (Yeh et al., 2017). This allows Cre-mediated excision of the floxed region resulting in a knock-out allele. Nalcn$^{FL/FL}$ mice

were injected with an AAV9 virus carrying Cre-recombinase (Addgene plasmid # 49056) with a human synapsin promoter to limit expression to neurons (Gompf et al., 2015). After waiting 4 weeks for the virus to express, our preliminary inspection of wide field fluorescence images, revealed clear Cre-driven EGFP fluorescence in the nuclei of neurons in the injected region. Two mice were injected off target with Cre being expressed in above the DR in the central gray and above that in the colliculi. Since Nalcn is expressed through the brain, immunohistochemistry was done to determine whether Nalcn expression was reduced in the area where Cre was expressed. Nalcn immunofluorescence did not appear to be strongly suppressed in the Cre-expressing regions. While some cells expressing Cre-recombinase, had little cytoplasmic staining for Nalcn, while other cells with Cre-expression showed substantial Nalcn staining. Since Nalcn, like other ion channels are expressed at rather low levels, we will next re-image the tissue sections to improve detectability of cellular fluorescence with the goal of counting the fraction of Cre-positive cells expressing Nalcn and compare this with the fraction of Cre-negative cells expressing Nalcn.

Afterwards, 3 more $Nalcn^{FL/FL}$ mice were injected with the AAV9-Cre virus. The Duration of Cre expression was different in each mouse, so we could see if longer exposure to Cre would provide better results since we are not sure how stable the Nalcn protein is which will dictate how long we need to wait before it is no longer present. Cre was expressed in the $Nalcn^{FL/FL}$ mice for 4, 6 and 8 weeks, before the mice were perfused. In the mice, in which Cre was expressed for 6 and 8 weeks, there was successfully expression with Cre expression in the Dorsal Raphe (**Figure 19A**). However, even with the 8-week Cre expression, we saw the same pattern of Cre+ cells with Nalcn

immunoreactivity and other Cre+ cells without Nalcn immunoreactivity (**Figure 19B**). This could mean that antibody staining is not reflecting the Nalcn protein levels or that the half-life of the channels is extremely long. To determine that we are actually knocking down Nalcn mRNA expression, in future experiments we will prepare tissue punches from AAV-injected mice, centered on the injection (determined by Cre-fluorescence) and adjacent regions to compare Nalcn mRNA levels by qRT-PCR.

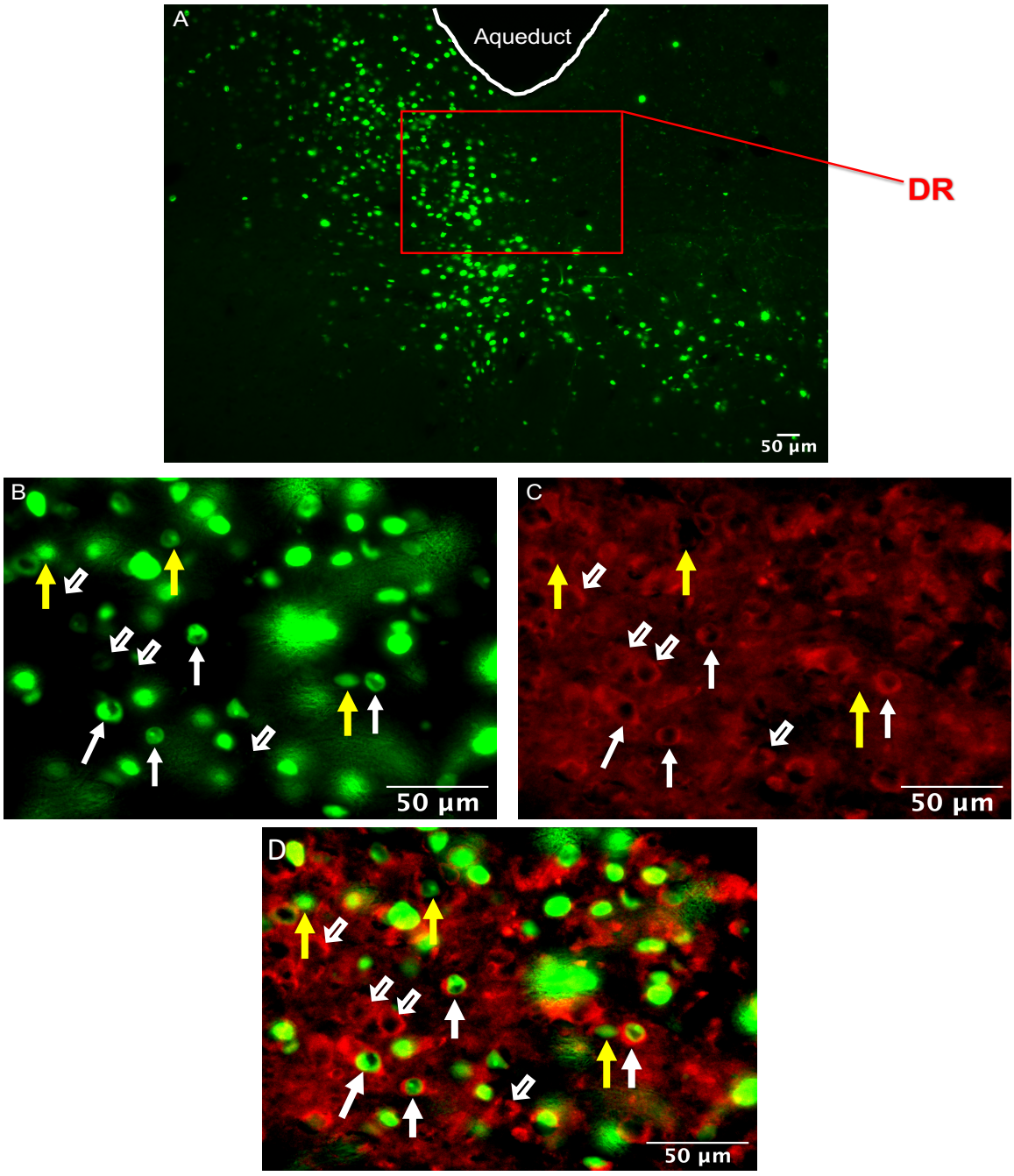


**Figure 19 | Cre expression produced by AAV9-hSyn-eGFP-Cre microinjection in Nalcn$^{FL/FL}$ 8-weeks after microinjection**
**(A)** nuclear expression of EGFP-Cre extends into the DR (10x obj). **(B)** Higher magnification of EGFP-Cre expression in the DR (60x obj). **(C)** Nalcn immunostaining in the DR. **(D)** Merge of EGFP-Cre and Nalcn immunostaining. In B-D, the white solid arrows indicate some cells with EGFP nuclei and Nalcn immunostaining. Yellow arrow heads indicate cells with EGFP-Cre+ and no Nalcn+ cytoplasm; Open white arrows indicate Nalcn+ cytoplasm lacking EGFP-Cre+ nuclei.

**Discussion**

Based on function expression studies, many genes code for subunits that form functional ion channels with properties similar to the cation channel effectors in 5-HT DR neurons. These include many members of the Trp superfamily of ion channels and the Nalcn channel. Purkinje neurons were chosen for comparison, because despite having different electrical properties and no reported direct orexin responses, they have several types of cation permeable ion channels. Half the serotonergic neurons analyzed were obtained from the median raphe (MR) and half from the dorsal raphe. This was done to get a wider range of genes expressed by 5-HT neurons and because DR and MR containing neurons have similar responses to orexin. This was confirmed when we saw a similar expression pattern of most genes in the dorsal and median raphe neurons. In the last year more sets of scRNA-seq data from just the DR have been made available so it will be interesting to re-run this analysis with more 5-HT DR cells to see if other subunits are detected from a wider pool of cells.

Initially, the gene expression profile of 30,244 genes were analyzed. We then used the AmiGO2 database to construct a broad list of channel genes that might be influenced by orexin receptor activation and performed single cell RNA sequence analysis on each group. After analyzing the gene expression profiles of multiple groups of channels, we isolated 39 genes (**Figure 12**) that we thought could be potential candidates based on their novel orexin actions. One thing we noted was that there was a clear distinction between serotonergic neurons and cerebellar Purkinje neurons based on the gene expression profiles of the selected channels, which could be visualized by the tSNE plot (**Figure 4**). These

differences likely contribute to the underlying electrophysiological differences between these cell types.

Several interesting channels were noted including the Asic channels, which were differentially expressed in DR neurons and are cation channels. Panx1 is another channel of interest, which makes a massive conductance single channel that is permeable to all kinds of things including small second messenger molecules like adenosine. Another channel of interest was the Kcnd3 or Kv.4.3 channel, which was highly expressed in the DR. These channels produce an A-type $K^+$ current and is the likely identity of the orexin inhibited A-current that was previously described in DR neurons (Ishibashi et al, 2016) and other GPCRs in other cells, including dopamine cells (Gantz & Bean, 2017).

The next group of channels we consider candidates for the orexin activated cation channel included TRPC3, 6, and 7. It is known that Trpc3, 6, and 7 that can hetero-multimerize and form functional channels. Even though Trpc3 is more differentially expressed in Purkinje cells on average than it is in the raphe neurons and Trpc6 isn't expressed much in either neurons, it is possible that Trpc7 is forms homomeric channels, which could account for the current we have seen following orexin application. One appeal of TRPC channels is that produce very noisy currents which would fit with the noisiness we see when the cation current gets turned on by orexin and the decreasing noise during the oeAHP. Another interesting thing is that they are known to be inhibited by intracellular calcium. One potential problem with this idea is that the TRPC channels are calcium permeable, which has been difficult to demonstrate in DR neurons (Kohlmeier et al., 2008).

Given the many possible candidates we chose to first test Nalcn. This decision was based on our previous laboratory research done on orexin actions on DR neurons. Nalcn is part of a complex which includes GPCRs and might be considered a GPCR-activated channel (Cochet-Bissuel et al., 2014). Since orexin receptors can efficiently couple to PLC (Kukkonen & Leonard, 2013) it is possible that Nalcn is one effector. Nalcn is also highly sodium selective and doesn't effectively permeate calcium as suggested for the orexin current in DR (Kohlmeier et al., 2008). Nalcn is also inhibited by extracellular calcium (Lee et al., 2019) at above physiological levels, which is similar to the current that is activated by Orexin (Ishibashi and Leonard, unpublished observations). Finally, the availability of $Nalcn^{FL/FL}$ mice and a possible antibody for Nalcn were also factors in selecting Nalcn as the first candidate to test.

Using a [1:100] dilution of anti-Nalcn antibody we found Nalcn immunostaining in serotonergic neurons of the DR in Sert-Cre/dTom mice (**Figure 16C**). From this we might conclude this is convincing immunocytochemistry supporting the idea that Nalcn is expressed in serotonergic neurons among other neurons of the DR.

To further test this idea, we attempted to knock out Nalcn expression by expressing Cre into the DR of mice that have the Nalcn gene floxed. We saw that the Cre expression was nuclear in nature based on the EGFP tag, suggesting it was properly expressed at our target sites. However, there did not appear to be the expected dramatic loss of Nalcn immunofluorescence. This suggests that the channel protein is either persistent for more than 8 weeks following injection or the immunostaining, or that the immunofluorescence is not reflecting Nalcn protein levels.

To further explore this, we can try expressing Cre in Nalcn$^{FL/FL}$ mice for longer than 8 weeks to see if there is a reduction of Nalcn immunofluorescence. We can check also the message levels to see if there is a reduction Nalcn mRNA. Finally, we can try additional antibodies or use whole cell patch clamping in brain slices to functionally test if Nalcn is functionally absent in cells expressing Cre-EGFP in DR neurons. Assuming we can prove we have knocked out the channel we can then use patch clamp methods to determine if orexin still has its complex actions in the absence of Nalcn. Of course, it is possible that Nalcn is not the correct channel, in which case, this same approach can be performed with another candidate channel identified using bioinformatics, such as Trpc7.

Assuming we can demonstrate a knock-down of Nalcn, we will then use whole cell patch clamping in brain slices to functionally test if Nalcn is the channel that mediates the Orexin A action on serotonergic neurons of DR. It is possible that Nalcn is not the correct channel, in which case, this same approach can be performed with another candidate channel identified using bioinformatics (e.g., Trpc3/7). Even if Nalcn is not the channel that mediates the Orexin A action, it is likely that a 5-HT neuron specific knockout of Nalcn will affect the resting potential of DR-5-HT neurons. Further studies could be done to see the behavioral differences in the mice with Nalcn KO in these Serotonergic neurons of the DR.

We also noticed some limitations of this approach. We saw in the gene expression that Purkinje neurons appear not to have orexin (Hcrt) expression (**Figure 12),** so it is possible that the relevant channel is expressed in both cell types but is not activated by orexin in Purkinje cells. If this is the case, these cells wouldn't be detected by this analysis.

The channel we choose to test, Nalcn, does have some expression in Purkinje cells but it's not enough to be a significant upregulation.

**Bibliographic References**


**Aldrich, M. S.** (1998). Diagnostic aspects of narcolepsy. *Neurology*, *50*(2 Suppl 1), S2-7.

**Alexandre, C., Andermann, M. L., & Scammell, T. E.** (2013). Control of arousal by the orexin neurons. *Curr Opin Neurobiol*, *23*(5), 752-759.

**Azmitia, E. C., & Segal, M.** (1978). An autoradiographic analysis of the differential ascending projections of the dorsal and median raphe nuclei in the rat. *J Comp Neurol*, *179*(3), 641-667

B**assetti, C., & Aldrich, M. S.** (1996). Narcolepsy. *Neurol Clin*, *14*(3), 545-571.

**Batut, B., Hiltemann, S., Bagnacani, A., Baker, D., Bhardwaj, V., Blank, C., Bretaudeau, A., Brillet-Guéguen, L., Čech, M., Chilton, J., Clements, D., Doppelt-Azeroual, O., Erxleben, A., Freeberg, M. A., Gladman, S., Hoogstrate, Y., Hotz, H. R., Houwaart, T., Jagtap, P., Larivière, D., Le Corguillé, G., Manke, T., Mareuil, F., Ramírez, F., Ryan, D., Sigloch, F. C., Soranzo, N., Wolff, J., Videm, P., Wolfien, M., Wubuli, A., Yusuf, D., Taylor, J., Backofen, R., Nekrutenko, A., Grüning, B., & Network, G. T.** (2018). Community-Driven Data Analysis Training for Biology. *Cell Syst*, *6*(6), 752-758.e751.

**Bennett, K. M., Liu, J., Hoelting, C., & Stoll, J.** (2011). Expression and analysis of two novel rat organic cation transporter homologs, SLC22A17 and SLC22A23. *Mol Cell Biochem*, *352*(1-2), 143-154.

**Beusterien, K. M., Rogers, A. E., Walsleben, J. A., Emsellem, H. A., Reblando, J. A., Wang, L., Goswami, M., & Steinwald, B.** (1999). Health-related quality of life effects of modafinil for treatment of narcolepsy. *Sleep*, *22*(6), 757-765.

**Borgland, S. L., Taha, S. A., Sarti, F., Fields, H. L., & Bonci, A.** (2006). Orexin A in the VTA is critical for the induction of synaptic plasticity and behavioral sensitization to cocaine. *Neuron*, *49*(4), 589-601.

**Brodie, B. B., Pletscher, A., & Shore, P. A.** (1955). Evidence that serotonin has a role in brain function. *Science*, *122*(3177), 968.

**Brown, R. E., Sergeeva, O., Eriksson, K. S., & Haas, H. L.** (2001). Orexin A excites serotonergic neurons in the dorsal raphe nucleus of the rat. *Neuropharmacology*, *40*(3), 457-459.

**Brown, R. E., Sergeeva, O. A., Eriksson, K. S., & Haas, H. L.** (2002). Convergent excitation of dorsal raphe serotonin neurons by multiple arousal systems (orexin/hypocretin, histamine and noradrenaline). *J Neurosci*, *22*(20), 8850-8859.

B**urdakov, D., Jensen, L. T., Alexopoulos, H., Williams, R. H., Fearon, I. M., O'Kelly, I., Gerasimenko, O., Fugger, L., & Verkhratsky, A.** (2006). Tandem-pore K+ channels mediate inhibition of orexin neurons by glucose. *Neuron*, *50*(5), 711-722.

**Burlet, S., Tyler, C. J., & Leonard, C. S.** (2002). Direct and indirect excitation of laterodorsal tegmental neurons by Hypocretin/Orexin peptides: implications for wakefulness and narcolepsy. *J Neurosci*, *22*(7), 2862-2872.

**Burrell, B. D., & Crisp, K. M.** (2008). Serotonergic modulation of afterhyperpolarization in a neuron that contributes to learning in the leech. *J Neurophysiol*, *99*(2), 605-616.

**Byers, R. J., Hoyland, J. A., Dixon, J., & Freemont, A. J.** (2000). Subtractive hybridization--genetic takeaways and the search for meaning. *Int J Exp Pathol*, *81*(6), 391-404.

**Calva, C. B., Fayyaz, H., & Fadel, J. R.** (2018). Increased acetylcholine and glutamate efflux in the prefrontal cortex following intranasal orexin-A (hypocretin-1). *J Neurochem*, *145*(3), 232-244.

**Chemelli, R. M., Willie, J. T., Sinton, C. M., Elmquist, J. K., Scammell, T., Lee, C., Richardson, J. A., Williams, S. C., Xiong, Y., Kisanuki, Y., Fitch, T. E., Nakazato, M., Hammer, R. E., Saper, C. B., & Yanagisawa, M.** (1999). Narcolepsy in orexin knockout mice: molecular genetics of sleep regulation. *Cell*, *98*(4), 437-451.

**Cochet-Bissuel, M., Lory, P., & Monteil, A.** (2014). The sodium leak channel, NALCN, in health and disease. *Front Cell Neurosci*, *8*(132), 1-13.

**De Lecea, L., Kilduff, T. S., Peyron, C., Gao, X., Foye, P. E., Danielson, P. E., Fukuhara, C., Battenberg, E. L., Gautvik, V. T., Bartlett, F. S., Frankel, W. N., van den Pol, A. N., Bloom, F. E., Gautvik, K. M., & Sutcliffe, J. G.** (1998). The hypocretins: hypothalamus-specific peptides with neuroexcitatory activity. *Proc Natl Acad Sci U S A*, *95*(1), 322-327.

**Deng, Q., Ramsköld, D., Reinius, B., & Sandberg, R.** (2014). Single-cell RNA-seq reveals dynamic, random monoallelic gene expression in mammalian cells. *Science*, *343*(6167), 193-196.

**Duménieu, M., Fourcaud-Trocmé, N., Garcia, S., & Kuczewski, N.** (2015). Afterhyperpolarization (AHP) regulates the frequency and timing of action potentials in the mitral cells of the olfactory bulb: role of olfactory experience. *Physiol Rep*, *3*(5), 1-17.

**Ekholm, M. E., Johansson, L., & Kukkonen, J. P.** (2007). IP3-independent signalling of OX1 orexin/hypocretin receptors to Ca2+ influx and ERK. *Biochem Biophys Res Commun*, *353*(2), 475-480.

**Eriksson, K. S., Sergeeva, O., Brown, R. E., & Haas, H. L.** (2001). Orexin/hypocretin excites the histaminergic neurons of the tuberomammillary nucleus. *J Neurosci*, *21*(23), 9273-9279.

**Evans, C., Hardin, J., & Stoebel, D. M.** (2018). Selecting between-sample RNA-Seq normalization methods from the perspective of their assumptions. *Brief Bioinform*, *19*(5), 776-792.

**Gantz, S. C., & Bean, B. P.** (2017, Mar). Cell-Autonomous Excitation of Midbrain Dopamine Neurons by Endocannabinoid-Dependent Lipid Signaling. *Neuron*, 93(6), 1375-1387.e1372.

**Gartside, S. E., Cole, A. J., Williams, A. P., McQuade, R., & Judge, S. J.** (2007). AMPA and NMDA receptor regulation of firing activity in 5-HT neurons of the dorsal and median raphe nuclei. *Eur J Neurosci*, *25*(10), 3001-3008.

**Gautam, N., Downes, G. B., Yan, K., & Kisselev, O.** (1998). The G-protein betagamma complex. *Cell Signal*, *10*(7), 447-455.

**Gershon, M. D., & Brooks, D. C.** (1976). Monoamine oxidase inhibition and the induction of ponto-geniculo-occipital wave activity by reserpine in the cat. *J Pharmacol Exp Ther*, *197*(3), 556-566.

**Gompf, H. S., Budygin, E. A., Fuller, P. M., & Bass, C. E.** (2015). Targeted genetic manipulations of neuronal subtypes using promoter-specific combinatorial AAVs in wild-type animals. *Front Behav Neurosci*, *9*(152), 2-10.

**Gott, J. A., Liley, D. T., & Hobson, J. A.** (2017). Towards a Functional Understanding of PGO Waves. *Front Hum Neurosci*, *11*(89), 1-10.

**Goubert, E., Mircheva, Y., Lasorsa, F. M., Melon, C., Profilo, E., Sutera, J., Becq, H., Palmieri, F., Palmieri, L., Aniksztejn, L., & Molinari, F.** (2017). Inhibition of the Mitochondrial Glutamate Carrier SLC25A22 in Astrocytes Leads to Intracellular Glutamate Accumulation. *Front Cell Neurosci*, *11*(149), 2-12.

**Haque, A., Engel, J., Teichmann, S. A., & Lönnberg, T.** (2017). A practical guide to single-cell RNA-sequencing for biomedical research and clinical applications. *Genome Med*, *9*(75), 1-9.

**Hartmann, J., Dragicevic, E., Adelsberger, H., Henning, H. A., Sumser, M., Abramowitz, J., Blum, R., Dietrich, A., Freichel, M., Flockerzi, V., Birnbaumer, L., & Konnerth, A.** (2008). TRPC3 channels are required for synaptic transmission and motor coordination. *Neuron*, *59*(3), 392-398.

**Hasegawa, E., Yanagisawa, M., Sakurai, T., & Mieda, M.** (2014). Orexin neurons suppress narcolepsy via 2 distinct efferent pathways. *J Clin Invest*, *124*(2), 604-616.

**Hepler, J. R., & Gilman, A. G.** (1992). G proteins. *Trends Biochem Sci*, *17*(10), 383-387.

**Hirai, N., & Nishino, S.** (2011). Recent advances in the treatment of narcolepsy. *Curr Treat Options Neurol*, *13*(5), 437-457.

**Hofmann, F.** (2018). PKC and calcium channel trafficking. *Channels (Austin)*, *12*(1), 15-16.

**Hollt, T., Pezzotti, N., van Unen, V., Koning, F., Lelieveldt, B. P. F., & Vilanova, A.** (2018). CyteGuide: Visual Guidance for Hierarchical Single-Cell Analysis. *IEEE Trans Vis Comput Graph*, *24*(1), 739-748.

**Hondo, M., Nagai, K., Ohno, K., Kisanuki, Y., Willie, J. T., Watanabe, T., Yanagisawa, M., & Sakurai, T.** (2010). Histamine-1 receptor is not required as a downstream effector of orexin-2 receptor in maintenance of basal sleep/wake states. *Acta Physiol (Oxf)*, *198*(3), 287-294.

**Horvath, T. L., Peyron, C., Diano, S., Ivanov, A., Aston-Jones, G., Kilduff, T. S., & van Den Pol, A. N.** (1999). Hypocretin (orexin) activation and synaptic innervation of the locus coeruleus noradrenergic system. *J Comp Neurol*, *415*(2), 145-159.

**Hwang, L. L., Chen, C. T., & Dun, N. J.** (2001). Mechanisms of orexin-induced depolarizations in rat dorsal motor nucleus of vagus neurones in vitro. *J Physiol*, *537*(Pt 2), 511-520.

**Inutsuka, A., & Yamanaka, A.** (2013). The physiological role of orexin/hypocretin neurons in the regulation of sleep/wakefulness and neuroendocrine functions. *Front Endocrinol (Lausanne)*, *4*(18), 1-7.

**Ishibashi, M., Gumenchuk, I., Miyazaki, K., Inoue, T., Ross, W. N., & Leonard, C. S.** (2016). Hypocretin/Orexin Peptides Alter Spike Encoding by Serotonergic Dorsal Raphe Neurons through Two Distinct Mechanisms That Increase the Late Afterhyperpolarization. *J Neurosci*, *36*(39), 10097-10115.

**Jacobs, B. L., & Fornal, C. A.** (1999). Activity of serotonergic neurons in behaving animals. *Neuropsychopharmacology*, *21*(2 Suppl), 9S-15S.

**James, G., Witten, D., Hastie, T., Tibshirani, R., & Ebscohost.** (2013). *An introduction to statistical learning : with applications in R* (Uncorrected edition . ed.). Springer.

**Jouvet, M.** (1968). Insomnia and decrease of cerebral 5-hydroxytryptamine after destruction of the raphe system in the cat. *Adv Pharmacol*, *6*(Pt B), 265-279.

**Jouvet-Mounier, D., Vimont, P., & Delorme, F.** (1965). [Study of the effects of sleep deprivation in the adult cat]. *J Physiol (Paris)*, *57*(5), 636-637.

**Kang, D., Choe, C., & Kim, D.** (2005). Thermosensitivity of the two-pore domain K+ channels TREK-2 and TRAAK. *J Physiol*, *564*(Pt 1), 103-116.

**Kang, G., Joseph, J. W., Chepurny, O. G., Monaco, M., Wheeler, M. B., Bos, J. L., Schwede, F., Genieser, H. G., & Holz, G. G.** (2003). Epac-selective cAMP analog 8-pCPT-2'-O-Me-cAMP as a stimulus for Ca2+-induced Ca2+ release and exocytosis in pancreatic beta-cells. *J Biol Chem*, *278*(10), 8279-8285.

**Kim, J. K., Kolodziejczyk, A. A., Ilicic, T., Illicic, T., Teichmann, S. A., & Marioni, J. C.** (2015). Characterizing noise structure in single-cell RNA-seq distinguishes genuine from technical stochastic allelic expression. *Nat Commun*, *6*(8687), 2-8.

**Koella, W. P., Feldstein, A., & Czicman, J. S.** (1968). The effect of para-chlorophenylalanine on the sleep of cats. *Electroencephalogr Clin Neurophysiol*, *25*(5), 481-490.

**Kohlmeier, K. A., Inoue, T., & Leonard, C. S.** (2004). Hypocretin/orexin peptide signaling in the ascending arousal system: elevation of intracellular calcium in the mouse dorsal raphe and laterodorsal tegmentum. *J Neurophysiol*, *92*(1), 221-235.

**Kohlmeier, K. A., Watanabe, S., Tyler, C. J., Burlet, S., & Leonard, C. S.** (2008). Dual orexin actions on dorsal raphe and laterodorsal tegmentum neurons: noisy cation current activation and selective enhancement of Ca2+ transients mediated by L-type calcium channels. *J Neurophysiol*, *100*(4), 2265-2281.

**Kukkonen, J. P., & Leonard, C. S.** (2013). Orexin/hypocretin receptor signalling cascades. *Br J Pharmacol*, *171*(2), 314-331.

**Lambe, E. K., Olausson, P., Horst, N. K., Taylor, J. R., & Aghajanian, G. K.** (2005). Hypocretin and nicotine excite the same thalamocortical synapses in prefrontal cortex: correlation with improved attention in rat. *J Neurosci*, *25*(21), 5225-5229.

**Lee, S. Y., Vuong, T. A., Wen, X., Jeong, H. J., So, H. K., Kwon, I., Kang, J. S., & Cho, H.** (2019). Methylation determines the extracellular calcium sensitivity of the leak channel NALCN in hippocampal dentate granule cells. *Exp Mol Med*, *51*(10), 1-14.

**Leibowitz, S. F., & Alexander, J. T.** (1998). Hypothalamic serotonin in control of eating behavior, meal size, and body weight. *Biol Psychiatry*, *44*(9), 851-864.

**Leonard, C. S., & Kukkonen, J. P.** (2013). Orexin/hypocretin receptor signalling: a functional perspective. *Br J Pharmacol*, *171*(2), 294-313.

**Li, Y., Gao, X. B., Sakurai, T., & van den Pol, A. N.** (2002). Hypocretin/Orexin excites hypocretin neurons via a local glutamate neuron-A potential mechanism for orchestrating the hypothalamic arousal system. *Neuron*, *36*(6), 1169-1181.

**Li, Y., Zhong, W., Wang, D., Feng, Q., Liu, Z., Zhou, J., Jia, C., Hu, F., Zeng, J., Guo, Q., Fu, L., & Luo, M.** (2016). Serotonin neurons in the dorsal raphe nucleus encode reward signals. *Nat Commun*, *7*(10503), 2-13.

**Lin, L., Faraco, J., Li, R., Kadotani, H., Rogers, W., Lin, X., Qiu, X., de Jong, P. J., Nishino, S., & Mignot, E.** (1999). The sleep disorder canine narcolepsy is caused by a mutation in the hypocretin (orexin) receptor 2 gene. *Cell*, *98*(3), 365-376.

**Liu, R. J., van den Pol, A. N., & Aghajanian, G. K.** (2002). Hypocretins (orexins) regulate serotonin neurons in the dorsal raphe nucleus by excitatory direct and inhibitory indirect actions. *J Neurosci*, *22*(21), 9453-9464.

**Lytal, N., Ran, D., & An, L.** (2020). Normalization Methods on Single-Cell RNA-seq Data: An Empirical Survey. *Front Genet*, *11*(41), 1-13.

**Mahoney, C. E., Cogswell, A., Koralnik, I. J., & Scammell, T. E.** (2019). The neurobiological basis of narcolepsy. *Nat Rev Neurosci*, *20*(2), 83-93.

**Marcus, J. N., Aschkenasi, C. J., Lee, C. E., Chemelli, R. M., Saper, C. B., Yanagisawa, M., & Elmquist, J. K.** (2001). Differential expression of orexin receptors 1 and 2 in the rat brain. *J Comp Neurol*, *435*(1), 6-25.

**McGinty, D. J., & Harper, R. M.** (1976). Dorsal raphe neurons: depression of firing during sleep in cats. *Brain Res*, *101*(3), 569-575.

**Nakamura, K.** (2013). The role of the dorsal raphé nucleus in reward-seeking behavior. *Front Integr Neurosci*, *7*(60), 1-12.

**Naylor, E., Aillon, D. V., Barrett, B. S., Wilson, G. S., Johnson, D. A., Harmon, H. P., Gabbert, S., & Petillo, P. A.** (2012). Lactate as a biomarker for sleep. *Sleep*, *35*(9), 1209-1222.

**Negrini, D., Marcozzi, C., Solari, E., Bossi, E., Cinquetti, R., Reguzzoni, M., & Moriondo, A.** (2016). Hyperpolarization-activated cyclic nucleotide-gated channels in peripheral diaphragmatic lymphatics. *Am J Physiol Heart Circ Physiol*, *311*(4), H892-H903.

**Nishino, S., & Mignot, E.** (1997). Pharmacological aspects of human and canine narcolepsy. *Prog Neurobiol*, *52*(1), 27-78.

**Okaty, B. W., Freret, M. E., Rood, B. D., Brust, R. D., Hennessy, M. L., deBairos, D., Kim, J. C., Cook, M. N., & Dymecki, S. M.** (2015). Multi-Scale Molecular Deconstruction of the Serotonin Neuron System. *Neuron*, *88*(4), 774-791.

**Pagnuco, I. A., Pastore, J. I., Abras, G., Brun, M., & Ballarin, V. L.** (2017). Analysis of genetic association using hierarchical clustering and cluster validation indices. *Genomics*, *109*(5-6), 438-445.

**Park, J. H., Shim, H. M., Na, A. Y., Bae, J. H., Im, S. S., & Song, D. K.** (2015). Orexin A regulates plasma insulin and leptin levels in a time-dependent manner following a glucose load in mice. *Diabetologia*, *58*(7), 1542-1550.

**Parsons, M. P., Belanger-Willoughby, N., Linehan, V., & Hirasawa, M.** (2012). ATP-sensitive potassium channels mediate the thermosensory response of orexin neurons. *J Physiol*, *590*(19), 4707-4715.

**Parsons, M. P., & Hirasawa, M.** (2010). ATP-sensitive potassium channel-mediated lactate effect on orexin neurons: implications for brain energetics during arousal. *J Neurosci*, *30*(24), 8061-8070.

**Peltonen, H. M., Magga, J. M., Bart, G., Turunen, P. M., Antikainen, M. S., Kukkonen, J. P., & Akerman, K. E.** (2009). Involvement of TRPC3 channels in calcium oscillations mediated by OX(1) orexin receptors. *Biochem Biophys Res Commun*, *385*(3), 408-412.

**Peyron, C., Tighe, D. K., van den Pol, A. N., de Lecea, L., Heller, H. C., Sutcliffe, J. G., & Kilduff, T. S.** (1998). Neurons containing hypocretin (orexin) project to multiple neuronal systems. *J Neurosci*, *18*(23), 9996-10015.

**Pintwala, S., & Peever, J.** (2017). Circuit mechanisms of sleepiness and cataplexy in narcolepsy. *Curr Opin Neurobiol*, *44*, 50-58.

**Pizza, F., Antelmi, E., Vandi, S., Meletti, S., Erro, R., Baumann, C. R., Bhatia, K. P., Dauvilliers, Y., Edwards, M. J., Iranzo, A., Overeem, S., Tinazzi, M., Liguori, R., & Plazzi, G.** (2018). The distinguishing motor features of cataplexy: a study from video-recorded attacks. *Sleep*, *41*(5).

**Plant, T. D., & Schaefer, M.** (2003). TRPC4 and TRPC5: receptor-operated Ca2+-permeable nonselective cation channels. *Cell Calcium*, *33*(5-6), 441-450.

**Puliti, A., Caridi, G., Ravazzolo, R., & Ghiggeri, G. M.** (2007). Teaching molecular genetics: chapter 4-positional cloning of genetic disorders. *Pediatr Nephrol*, *22*(12), 2023-2029.

**Putula, J., Pihlajamaa, T., & Kukkonen, J. P.** (2014). Calcium affects OX1 orexin (hypocretin) receptor responses by modifying both orexin binding and the signal transduction machinery. *Br J Pharmacol*, *171*(24), 5816-5828.

**Raifman, T. K., Kumar, P., Haase, H., Klussmann, E., Dascal, N., & Weiss, S.** (2017). Protein kinase C enhances plasma membrane expression of cardiac L-type calcium channel, Ca. *Channels (Austin)*, *11*(6), 604-615.

**Reading, P.** (2019). Cataplexy. *Pract Neurol*, *19*(1), 21-27.

**Ren, J., Isakova, A., Friedmann, D., Zeng, J., Grutzner, S. M., Pun, A., Zhao, G. Q., Kolluru, S. S., Wang, R., Lin, R., Li, P., Li, A., Raymond, J. L., Luo, Q., Luo, M., Quake, S. R., & Luo, L.** (2019). Single-cell transcriptomes and whole-brain projections of serotonin neurons in the mouse dorsal and median raphe nuclei. *Elife*, *8*, 1-29.

**Sakurai, T.** (2007). The neural circuit of orexin (hypocretin): maintaining sleep and wakefulness. *Nat Rev Neurosci*, *8*(3), 171-181.

**Sakurai, T., Amemiya, A., Ishii, M., Matsuzaki, I., Chemelli, R. M., Tanaka, H., Williams, S. C., Richarson, J. A., Kozlowski, G. P., Wilson, S., Arch, J. R., Buckingham, R. E., Haynes, A. C., Carr, S. A., Annan, R. S., McNulty, D. E., Liu, W. S., Terrett, J. A., Elshourbagy, N. A., Bergsma, D. J., & Yanagisawa, M.** (1998). Orexins and orexin receptors: a family of hypothalamic neuropeptides and G protein-coupled receptors that regulate feeding behavior. *Cell*, *92*(5), 573-585.

**Samanta, A., Hughes, T. E. T., & Moiseenkova-Bell, V. Y.** (2018). Transient Receptor Potential (TRP) Channels. *Subcell Biochem*, *87*, 141-165.

**Selbach, O., Doreulee, N., Bohla, C., Eriksson, K. S., Sergeeva, O. A., Poelchen, W., Brown, R. E., & Haas, H. L.** (2004). Orexins/hypocretins cause sharp wave- and theta-related synaptic plasticity in the hippocampus via glutamatergic, gabaergic, noradrenergic, and cholinergic signaling. *Neuroscience*, *127*(2), 519-528.

**Serôdio, P., & Rudy, B.** (1998). Differential expression of Kv4 K+ channel subunits mediating subthreshold transient K+ (A-type) currents in rat brain. *J Neurophysiol*, *79*(2), 1081-1091.

**Song, M. Y., & Yuan, J. X.** (2010). Introduction to TRP channels: structure, function, and regulation. *Adv Exp Med Biol*, *661*, 99-108.

**Tasoulis, D. K., Plagianakos, V. P., & Vrahatis, M. N.** (2006). Unsupervised clustering in mRNA expression profiles. *Comput Biol Med*, *36*(10), 1126-1142.

**Teixeira, V. G., Faccenda, J. F., & Douglas, N. J.** (2004). Functional status in patients with narcolepsy. *Sleep Med*, *5*(5), 477-483.

**Tjondrokoesoemo, A., Li, N., Lin, P. H., Pan, Z., Ferrante, C. J., Shirokova, N., Brotto, M., Weisleder, N., & Ma, J.** (2013). Type 1 inositol (1,4,5)-trisphosphate receptor activates ryanodine receptor 1 to mediate calcium spark signaling in adult mammalian skeletal muscle. *J Biol Chem*, *288*(4), 2103-2109.

**Torrealba, F., Yanagisawa, M., & Saper, C. B.** (2003). Colocalization of orexin a and glutamate immunoreactivity in axon terminals in the tuberomammillary nucleus in rats. *Neuroscience*, *119*(4), 1033-1044.

**Trebak, M., Lemonnier, L., Smyth, J. T., Vazquez, G., & Putney, J. W.** (2007). Phospholipase C-coupled receptors and activation of TRPC channels. *Handb Exp Pharmacol*(179), 593-614.

**Treutlein, B., Brownfield, D. G., Wu, A. R., Neff, N. F., Mantalas, G. L., Espinoza, F. H., Desai, T. J., Krasnow, M. A., & Quake, S. R.** (2014). Reconstructing lineage hierarchies of the distal lung epithelium using single-cell RNA-seq. *Nature*, *509*(7500), 371-375.

**Tsuboi, T., da Silva Xavier, G., Holz, G. G., Jouaville, L. S., Thomas, A. P., & Rutter, G. A.** (2003). Glucagon-like peptide-1 mobilizes intracellular Ca2+ and stimulates mitochondrial ATP synthesis in pancreatic MIN6 beta-cells. *Biochem J*, *369*(Pt 2), 287-299.

**Vallejos, C. A., Marioni, J. C., & Richardson, S.** (2015). BASiCS: Bayesian Analysis of Single-Cell Sequencing Data. *PLoS Comput Biol*, *11*(6), e1004333.

**Wada, H., Inagaki, N., Yamatodani, A., & Watanabe, T.** (1991). Is the histaminergic neuron system a regulatory center for whole-brain activity? *Trends Neurosci*, *14*(9), 415-418.

**Wang, C., Wang, Q., Ji, B., Pan, Y., Xu, C., Cheng, B., Bai, B., & Chen, J.** (2018). The Orexin/Receptor System: Molecular Mechanism and Therapeutic Potential for Neurological Diseases. *Front Mol Neurosci*, *11*(220), 1-11.

**Wang, Z., Liu, S., Kakizaki, M., Hirose, Y., Ishikawa, Y., Funato, H., Yanagisawa, M., Yu, Y., & Liu, Q.** (2014). Orexin/hypocretin activates mTOR complex 1 (mTORC1) via an Erk/Akt-independent and calcium-stimulated lysosome v-ATPase pathway. *J Biol Chem*, *289*(46), 31950-31959.

**Willie, J. T., Chemelli, R. M., Sinton, C. M., Tokita, S., Williams, S. C., Kisanuki, Y. Y., Marcus, J. N., Lee, C., Elmquist, J. K., Kohlmeier, K. A., Leonard, C. S., Richardson, J. A., Hammer, R. E., & Yanagisawa, M.** (2003). Distinct narcolepsy syndromes in Orexin receptor-2 and Orexin null mice: molecular genetic dissection of Non-REM and REM sleep regulatory processes. *Neuron*, *38*(5), 715-730.

**Wu, X., Liao, L., Liu, X., Luo, F., Yang, T., & Li, C.** (2012). Is ZD7288 a selective blocker of hyperpolarization-activated cyclic nucleotide-gated channel currents? *Channels (Austin)*, *6*(6), 438-442.

**Yamanaka, A., Muraki, Y., Tsujino, N., Goto, K., & Sakurai, T.** (2003). Regulation of orexin neurons by the monoaminergic and cholinergic systems. *Biochem Biophys Res Commun*, *303*(1), 120-129.

**Yeh, S. Y., Huang, W. H., Wang, W., Ward, C. S., Chao, E. S., Wu, Z., Tang, B., Tang, J., Sun, J. J., Esther van der Heijden, M., Gray, P. A., Xue, M., Ray, R. S., Ren, D., & Zoghbi, H. Y.** (2017). Respiratory Network Stability and Modulatory Response to Substance P Require Nalcn. *Neuron*, *94*(2), 294-303.e294.

**Zawilska, J. B., Woldan-Tambor, A., Płocka, A., Kużajska, K., & Wojcieszak, J.** (2012). [Narcolepsy: etiology, clinical features, diagnosis and treatment]. *Postepy Hig Med Dosw (Online)*, *66*, 771-786.

**Zhu, Y., Miwa, Y., Yamanaka, A., Yada, T., Shibahara, M., Abe, Y., Sakurai, T., & Goto, K.** (2003). Orexin receptor type-1 couples exclusively to pertussis toxin-

insensitive G-proteins, while orexin receptor type-2 couples to both pertussis toxin-sensitive and -insensitive G-proteins. *J Pharmacol Sci*, *92*(3), 259-266.

# Appendix

| Gene name | Description | Phenotype Overview | Molecular function | Biological process | Cellular component |
|---|---|---|---|---|---|
| Cacna2d1 | VGCC, alpha2/delta subunit 1 | **Behavior/neurological**, **homeostasis**/metabolism, muscle, cardiovascular, hematopoietic, renal/urinary and **nervous system** | Transporter | establishment of localization, homeostatic process, response to stimulus, signaling | endoplasmic reticulum, plasma membrane, synapse |
| Cacna1b | pore forming, VGCC, N type, alpha 1B subunit | **Behavior/neurological**, growth/size/body, **homeostasis**/metabolism, integument, mortality/aging, cardiovascular and **nervous system** | carbohydrate derivative binding, transporter | establishment of localization, response to stimulus, signaling | Cell projection, plasma membrane, synapse |
| Cacna1e | pore forming, VGCC, R type, alpha 1E subunit | **Behavior/neurological,** endocrine/exocrine glands, growth/size/body, **homeostasis**/metabolism, **nervous system** | transporter | establishment of localization, homeostatic process, response to stimulus, signaling | plasma membrane, synapse |
| Cacng3 | VGCC, gamma subunit 3 | **homeostasis**/metabolism | **Signaling receptor binding**, transporter | establishment of localization, response to stimulus, signaling | Cell projection, plasma membrane, synapse |
| Cacna1c | VGCC, L type, alpha 1C subunit | **behavior/neurological**, cellular, craniofacial, embryo, endocrine/exocrine glands, growth/size/body, **homeostasis**/metabolism, integument, mortality/aging, muscle, hematopoietic, immune, cardiovascular and **nervous system** | cytoskeletal protein binding, transporter | establishment of localization, homeostatic process, immune system process, response to stimulus, signaling, system development | Cell projection, non-membrane-bounded organelle, plasma membrane, synapse |
| Cacnb1 | VGCC, beta 1 subunit | **behavior/neurological,** limbs/digits/tail, mortality/aging muscle, skeleton | transporter | cellular component organization, establishment of localization, response to stimulus, signaling | endoplasmic reticulum, plasma membrane, synapse |
| Cacna1a | Pore forming, VGCC, P/Q type, alpha 1A subunit | **behavior/neurological,** cellular, endocrine/exocrine glands growth/size/body, **homeostasis**/metabolism, integument, mortality/aging, muscle, immune, hematopoietic, reproductive, respiratory, and **nervous system** | transporter | cell death, cell differentiation, cellular component organization, establishment of localization, homeostatic process, response to stimulus, signaling, system development | Cell projection, nucleus, plasma membrane, synapse |

**Table 1 | Description of potential candidate $Ca^{2+}$ genes**
The phenotype overview column indicates any direct phenotypes attributed to mutations/alleles of the gene. Green labels indicate potential candidate genes with novel orexin actions. The cellular component refers to the location relative to cellular structures in which the channel performs a function. All data was obtained from Ensembl and mouse genome informatics database.

| Gene name | Description | Phenotype overview | Molecular function | Biological process | Cellular component |
|---|---|---|---|---|---|
| Grin2d | glutamate receptor, ionotropic, NMDA2D (epsilon 4) | behavior/neurological cardiovascular system, growth/size/body, homeostasis/metabolism, skeleton | Signaling receptor activity, transporter | establishment of localization, homeostatic process, response to stimulus, signaling | Plasma membrane, synapse |
| Grin2b | glutamate receptor, ionotropic, NMDA2B (epsilon 2) | behavior/neurological, mortality/aging, growth/size/body, homeostasis/metabolism, nervous system | signaling receptor activity, signaling receptor binding, transporter | Cell death, cellular component organization, establishment of localization, homeostatic process, protein metabolic process, response to stimulus, signaling, system development | cell projection, cytoplasmic vesicle, cytoskeleton, endosome, extracellular region, non-membrane-bounded organelle, plasma membrane, synapse, vacuole |
| Grin1 | glutamate receptor, ionotropic, NMDA1 (zeta 1) | behavior/neurological, cardiovascular system, cellular, growth/size/body, hearing/vestibular/ear, hematopoietic system, homeostasis/metabolism, mortality/aging, reproductive system, respiratory system, nervous system | signaling receptor activity, signaling receptor binding, transporter | Cell death, cell differentiation, cellular component organization, establishment of localization, homeostatic process, nucleic acid-templated transcription, protein metabolic process, response to stimulus, signaling, system development | cell projection, cytoplasmic vesicle, endoplasmic reticulum, extracellular region, plasma membrane, synapse |
| Grid1 | glutamate receptor, ionotropic, delta 1 | growth/size/body, hearing/vestibular/ear, skeleton, nervous system | signaling receptor activity, transporter | establishment of localization, signaling | Plasma membrane, synapse |
| Grm5 | glutamate receptor, metabotropic 5 | adipose tissue, behavior/neurological, growth/size/body, integument, nervous system | signaling receptor activity, signaling receptor binding | cell differentiation, cellular component organization, establishment of localization, nucleic acid-templated transcription, protein metabolic process, response to stimulus, signaling, system development | Cell projection, plasma membrane, synapse |
| Grik5 | glutamate receptor, ionotropic, kainate 5 | behavior/neurological, integument, nervous system | signaling receptor activity, transporter | Cell death, cellular component organization, establishment of localization, response to stimulus, signaling | Cell projection, endoplasmic reticulum, nucleus, organelle lumen, plasma membrane, synapse |
| Gria2 | glutamate receptor, ionotropic, AMPA2 (alpha 2) | behavior/neurological, cellular, growth/size/body, homeostasis/metabolism, integument, mortality/aging, nervous system | cytoskeletal protein binding, signaling receptor activity, signaling receptor binding, transporter | cellular component organization, establishment of localization, response to stimulus, signaling | cell projection, cytoplasmic vesicle, endoplasmic reticulum, extracellular region, plasma membrane, synapse |
| Grik2 | glutamate receptor, ionotropic, kainate 2 (beta 2) | behavior/neurological, growth/size/body, nervous system | signaling receptor activity, transporter | Cell death, establishment of localization, homeostatic process, response to stimulus, signaling | Cell projection, plasma membrane, synapse |

**Table 2 | Description of potential candidate glutamate genes**

The phenotype overview column indicates any direct phenotypes attributed to mutations/alleles of the gene. Green labels indicate potential candidate genes with novel orexin actions. The cellular component refers to the location relative to cellular structures in which the channel performs a function. All data was obtained from Ensembl and mouse genome informatics database.

| Gene name | Description | Phenotype | Molecular Function | Biological process | Cellular component |
|---|---|---|---|---|---|
| Hcrtr1 | hypocretin (orexin) receptor 1 | **behavior/neurological, nervous system** | **Signaling receptor activity** | Homoeostatic process, response to stimulus, signaling | Plasma membrane |
| Hcrtr2 | hypocretin (orexin) receptor 2 | **behavior/neurological,** muscle, **nervous system** | **Signaling receptor activity** | Homoeostatic process, response to stimulus, signaling | Plasma membrane |
| Ryr2 | ryanodine receptor 2 | **behavior/neurological**, cardiovascular system, embryo, endocrine/exocrine glands, growth/size/body, hematopoietic system, **homeostasis**/metabolism, immune system, mortality/aging, muscle, **nervous system** | Transporter | Cell death, establishment of localization, homeostatic process, response to stimulus, signaling, system development | cell projection, cytoplasmic vesicle, endoplasmic reticulum, non-membrane-bounded organelle, nucleus, organelle envelope, plasma membrane |

**Table 3 | Breakdown of potential candidate hypocretin and ryanodine genes**
The phenotype overview column indicates any direct phenotypes attributed to mutations/alleles of the gene. Green labels indicate potential candidate genes with novel orexin actions. The cellular component refers to the location relative to cellular structures in which the channel performs a function. All data was obtained from Ensembl and mouse genome informatics database.

| Gene name | Description | Phenotype overview | Molecular Function | Biological process | Cellular component |
|---|---|---|---|---|---|
| Trpv2 | transient receptor potential cation channel, subfamily V, member 2 | Cellular, growth/size/body, hematopoietic system, immune system, mortality/aging | Transporter | cell differentiation, cell population proliferation, cellular component organization, establishment of localization, homeostatic process, response to stimulus, system development | Cell projection, plasma membrane |
| Trpc7 | transient receptor potential cation channel, subfamily C, member 7 | Vision/eye | Transporter | establishment of localization, homeostatic process | Golgi apparatus, nucleus, plasma membrane |
| Trpm7 | transient receptor potential cation channel, subfamily M, member 7 | **behavior/neurological**, cellular, digestive/alimentary system, embryo, endocrine/exocrine glands, growth/size/body, hematopoietic system, **homeostasis**/metabolism, immune system, integument, mortality/aging, **nervous system**, pigmentation, renal/urinary system, vision/eye | carbohydrate derivative binding, cytoskeletal protein binding, transferase, transporter | Cell death, cellular component organization, establishment of localization, homeostatic process, protein metabolic process | cell projection, cytoplasmic vesicle, plasma membrane, synapse |
| Trpc4ap | transient receptor potential cation channel, subfamily C, member 4 associated protein | integument | N/A | protein metabolic process, system development | N/A |
| Trpc3 | transient receptor potential cation channel, subfamily C, member 3 | **behavior/neurological,** growth/size/body, hematopoietic system, immune system, mortality/aging, vision/eye, **nervous system** | Transporter | establishment of localization, homeostatic process, response to stimulus | Plasma membrane |
| Trpc6 | transient receptor potential cation channel, subfamily C, member 6 | **behavior/neurological**, cardiovascular system, **homeostasis**/metabolism, integument, muscle, renal/urinary system, vision/eye | cytoskeletal protein binding, transporter | cell differentiation, cellular component organization, establishment of localization, homeostatic process, protein metabolic process response to stimulus, system development | Plasma membrane |

**Table 4 | Breakdown of potential candidate TRP genes**
The phenotype overview column indicates any direct phenotypes attributed to mutations/alleles of the gene. All data was obtained from Ensembl and mouse genome informatics database. Green labels indicate potential candidate genes with novel orexin actions. Trpc6 is included because it forms heterodimer with Trpc3 and Trpc7.

| Gene name | Description | Phenotype | Molecular function | Biological process | Cellular component |
|---|---|---|---|---|---|
| Kcnk9 | potassium channel, subfamily K, member 9, task 3 | **Nervous system** | transporter | establishment of localization | cytoplasmic vesicle, plasma membrane, synapse |
| Kcnq3 | potassium voltage-gated channel, subfamily Q, member 3, M-current subunit | **behavior/neurological**, craniofacial, growth/size/body, **homeostasis**/metabolism, mortality/aging, **nervous system** | transporter | establishment of localization, response to stimulus | cell projection, plasma membrane |
| Kcnn3 | potassium intermediate/small conductance calcium-activated channel, subfamily N, member 3, SK3 | reproductive system respiratory system, mortality/aging, **nervous system** | Transporter | establishment of localization | cell projection, plasma membrane, synapse |
| Kcnq2 | potassium voltage-gated channel, subfamily Q, member 2, M-current subunit | **behavior/neurological,** growth/size/body, respiratory system, mortality/aging, **nervous system** | cytoskeletal protein binding | establishment of localization, signaling | cell projection, plasma membrane |
| Kcnq5 | potassium voltage-gated channel, subfamily Q, member 5, M-current subunit | mortality/aging, **nervous system** | Transporter | establishment of localization | plasma membrane |
| Kcnd3 | potassium voltage-gated channel, Shal-related family, member 3, Kv4.3 | adipose tissue, behavior/neurological, skeleton, growth/size/body | Transporter | cellular component organization, establishment of localization, response to stimulus, signaling | cell projection, endoplasmic reticulum, plasma membrane, synapse |

**Table 5 | Breakdown of potential candidate potassium genes**
The phenotype overview column indicates any direct phenotypes attributed to mutations/alleles of the gene. Green labels indicate potential candidate genes with novel orexin actions. The cellular component refers to the location relative to cellular structures in which the channel performs a function. All data was obtained from Ensembl and mouse genome informatics database.

| Gene name | Description | Phenotype overview | Molecular function | Biological process | Cellular component |
|---|---|---|---|---|---|
| **Slc6a4** | solute carrier family 6 (neurotransmitter transporter, serotonin), member 4 | behavior/neurological, cardiovascular, cellular, digestive/alimentary, endocrine/exocrine glands, growth/size/body, homeostasis/metabolism, integument, mortality/aging, muscle, nervous system | cytoskeletal protein binding, transporter | cell differentiation, cell population proliferation, establishment of localization, response to stimulus, signaling, system development | cell projection, cytoplasmic vesicle, endosome, plasma membrane, synapse |
| Slc22a3 | solute carrier family 22 (organic cation transporter), member 3, extra neuronal monoamine transporter | Cellular, hematopoietic system, homeostasis/metabolism, immune system, nervous system, vision/eye | transporter | establishment of localization, response to stimulus | Plasma membrane |
| **Slc22a17** | solute carrier family 22 (organic cation transporter), member 17, cell surface receptor for LCN2 (24p3) | behavior/neurological, Limbs/digits/tail, mortality/aging, skeleton | Signaling receptor activity, transporter | establishment of localization, homeostatic process | Plasma membrane, vacuole |
| Slc22a23 | solute carrier family 22, member 23 | N/A | transporter | establishment of localization | N/A |
| Slc25a22 | solute carrier family 25 (mitochondrial carrier, glutamate), member 22 | N/A | transporter | establishment of localization | Mitochondrion, organelle envelope |

**Table 6 | Breakdown of potential solute carrier genes**
The phenotype overview column indicates any direct phenotypes attributed to mutations/alleles of the gene. Green labels indicate potential candidate genes with novel orexin actions. The cellular component refers to the location relative to cellular structures in which the channel performs a function. All data was obtained from Ensembl and mouse genome informatics database.

| Gene name | Description | Phenotype | Molecular function | Biological process | Cellular component |
|---|---|---|---|---|---|
| Hcn3 | hyperpolarization-activated, cyclic nucleotide-gated K+ 3 | cardiovascular system, **nervous system** | carbohydrate derivative binding, transporter | establishment of localization | cell projection, plasma membrane, synapse |
| Slc1a4 | solute carrier family 1 (glutamate/neutral amino acid transporter), member 4. Transporter for alanine, serine, cysteine, and threonine. Exhibits $Na^+$ dependance | growth/size/body, **homeostasis**/metabolism | Transporter | establishment of localization | Cell projection, cytoskeleton, non-membrane-bounded organelle, plasma membrane |
| Panx1 | Makes noisy current. Structural component of the gap junctions and the hemichannels involved in the ATP release and nucleotide permeation | **behavior/neurological**, cellular, hematopoietic system, **homeostasis**/metabolism, immune system, **nervous system**, respiratory system, vision/eye | cytoskeletal protein binding, signaling receptor binding, transporter | establishment of localization, response to stimulus, signaling | Cell projection, endoplasmic reticulum, plasma membrane |
| Trpc7 | transient receptor potential cation channel, subfamily C, member 7. Produces noisy cation current. | Vision/eye | transporter | establishment of localization, homeostatic process | Golgi apparatus, nucleus, plasma membrane |
| Asic2 | acid-sensing (proton-gated) ion channel 2 | cardiovascular system, hearing/vestibular/ear, muscle, **nervous system**, renal/urinary system, vision/eye | transporter | Cell death, cellular component organization, establishment of localization, response to stimulus, signaling, system development | Cell projection, plasma membrane, synapse |
| Nalcn | sodium leak channel, non-selective | **behavior/neurological**, cardiovascular system, growth/size/body, hematopoietic system, **homeostasis**/metabolism, immune system, mortality/aging, nervous system, renal/urinary system, respiratory system | transporter | establishment of localization | |
| Slc24a2 | solute carrier family 24 (sodium/potassium/calcium exchanger), member 2 | **behavior/neurological, homeostasis**/metabolism**, nervous system** | transporter | cellular component organization, establishment of localization, homeostatic process, signaling | Plasma membrane |

**Table 7 | Breakdown of Na or Ca dependent Non-Voltage gated ion channels**
The phenotype overview column indicates any direct phenotypes attributed to mutations/alleles of the gene. Green labels indicate potential candidate genes with novel orexin actions. The cellular component refers to the location relative to cellular structures in which the channel performs a function. All data was obtained from Ensembl and mouse genome informatics database.